Functionalized Protein Nanomaterials and their Biotechnological Applications

Benjamin Schmuck
Department of Molecular Science
Faculty of Natural Resources and Agricultural Sciences
Uppsala

Doctoral Thesis
Swedish University of Agricultural Sciences
Uppsala 2018

Acta Universitatis Agriculturae Sueciae
2018:57

ISSN 1652-6880
ISBN (print version) 978-91-7760-254-5
ISBN (electronic version) 978-91-7760-255-2

Print: SLU Service/Repro, Uppsala 2018

Functionalized Protein Nanomaterials and their Biotechnological Applications

Abstract

As the ribosomal synthesis of a nascent polypeptide progresses, the chain immediately undergoes folding into α-helical and β-strand secondary structure elements. While the protein matures, the polypeptide collapses into higher order constructs that ultimately form the native protein state. Since this state represents only a local minimum on the energy landscape of protein folding, the living cell has to continuously ensure an intact proteome through elaborate cellular mechanisms. However, some proteins have a high intrinsic propensity to escape these mechanisms and re-fold, which initiates protein aggregation into β-sheet rich protein nanofibrils (PNF).

The accumulation of PNF in living cells can be problematic and trigger a number of diseases. Nevertheless, some organisms utilize the robustness of these aggregates to build protective shells or to form biofilms. The insight that PNF fulfil physiological functions in nature, has led to the discovery of many, biotechnological useful, material properties. PNF based materials are environmentally friendly and can be specifically designed through genetic engineering. A diameter of less than 10 nm confers an enormous surface area over volume ratio to the nanofibrils. In addition, the fibrils have mechanical properties that are similar to spider dragline silk, natures 'high performance polymer'.

To exploit these properties biotechnologically, I aimed to solve critical challenges that delay real-world applications. First, I developed a strategy that allowed me to fibrillate the proteins Sup35 and Ure2 from *Saccharomyces cerevisiae* in a manner that ensures a maximal functionality of the active domains displayed on the surface of the nanofibrils. Second, I designed a set of biotechnological relevant fibrils to show that our fibrillation concept is universally applicable. Therefore, I assembled fibrils with an exceptional antibody binding capacity, antibiotic degrading properties, and compiled a reaction cascade of immobilized enzymes that process xylan biomass. Third, I characterized these functionalized fibrils in detail, which goes beyond the proof-of-concept stage. Fourth, I have raised an important question that concerns the choice of the proper methodology to upscale the production of PNF, to produce economical competitive products. As a first step towards this end goal, I used the methylotrophic yeast *Komagataella pastoris* as a host to produce ready-to-use fibrils, which can be separated from the yeast cells using centrifugation and water.

Still, additional major efforts are necessary to develop industrial-scale production methods. Another issue that awaits a solution, is the transfer of the nanofibril mechanical properties to macro-scale structures. To finally be able to close the gap between the laboratory to marketable product, a collaboration with industrial partners is required.

Keywords: functionalized nanofibrils, amyloid, protein-based materials, Sup35, Ure2

Author's address: Benjamin Schmuck, SLU, Department of Molecular Sciences, P.O. Box 7015, 750 07 Uppsala, Sweden
E-mail: benjamin.schmuck@slu.se

Dedication

To Alice, Joshua, and Joram

Contents

List of Publications

This thesis is based on the work contained in the following papers, referred to by Roman numerals in the text:

I **Benjamin Schmuck**, Mats Sandgren, and Torleif Härd* (2017). A fine-tuned composition of protein nanofibrils yields an upgraded functionality of displayed antibody binding domains. *Biotechnology Journal*, **16** (6)

II **Benjamin Schmuck**, Mats Sandgren, and Torleif Härd* (2018). The kinetics of TEM1 antibiotic degrading enzymes that are displayed on Ure2 protein nanofibrils in a flow reactor. *PLOS one*, **13** (4)

III **Benjamin Schmuck**, Mikael Gudmundsson, Johanna Blomqvist, Henrik Hansson, Torleif Härd, and Mats Sandgren* (2018). Production of ready-to-use functional Sup35 nanofibrils secreted by *Komagataella pastoris*. *ACS Nano*, **12** (9)

IV **Benjamin Schmuck**, Mikael Gudmundsson, Torleif Härd, and Mats Sandgren* (2018). Synergetic optimization of a xylan processing reaction cascade built from three enzymes immobilized on Sup35 nanofibrils. *Manuscript*.

Papers I-III are reproduced with the permission of the publishers.

* Corresponding author.

Additional Publications

V Elisabet Wahlberg, M. Mahafuzur Rahman, Hanna Lindberg, Elin Gunneriusson, **Benjamin Schmuck**, Christofer Lendel, Mats Sandgren, John Löfblom, Stefan Ståhl, and Torleif Härd* (2017). Identification of proteins that specifically recognize and bind protofibrillar aggregates of amyloid-β. *Scientific Reports*, **7** (1).

VI M. Mahafuzur Rahman, **Benjamin Schmuck**, Henrik Hansson, Gunilla T. Westermark, Torleif Härd, and Mats Sandgren* (2018). Enhanced detection of pathological ATTR aggregates using a nanofibril-based assay. *Manuscript*.

* Corresponding author.

The contribution of Benjamin Schmuck to the papers included in this thesis was as follows:

I Planned the work together with the co-authors, and executed all the laboratory work. Compiled and interpreted the data. Wrote the manuscript, assisted by the co-authors.

II Planned the work together with the co-authors, and executed all the laboratory work. Compiled and interpreted the data. Wrote the manuscript, assisted by the co-authors.

III Planned the work together with the co-authors. Executed the laboratory work together with the co-authors. Compiled and interpreted the data. Wrote the manuscript, assisted by the co-authors.

IV Planned the work together with the co-authors and performed the majority of the laboratory work. Compiled and interpreted the data. Wrote the manuscript, assisted by the co-authors.

Abbreviations

ASD	aldose sugar dehydrogenase
βXyl	β-xylosidase
E. coli	*Escherichia coli*
His_6	histidine tag
IMAC	immobilized metal ion affinity chromatography
IEX	ion exchange chromatography
IgG	immunoglobulin G
K. pastoris	*Komagataella pastoris*
kDa	kilo Dalton
mAB	monoclonal antibody
PNF	protein nano fibril
S. cerevisiae	*Saccharomyces cerevisiae*
SDS-PAGE	sodium dodecyl sulphate polyacrylamide gel electrophoresis
SPR	surface plasmon resonance
Sup35	translation release factor
TEM	transmission electron microscopy
ThT	thioflavin T
Ure2	ureidosuccinate transporter
XynA	xylanase A
ZZ	Z-domain dimer
DCIP	2,6-dichloroindophenol
MALDI-TOF	matrix assisted laser desorption ionization-time of flight mass spectrometry

1 Introduction

The advent of fully synthetic materials in the beginning of the 20th century (American Chemical Society, 2018), has triggered the development of material science. The versatility and low cost of plastics have led to an enormous variety of applications in industry, aerospace, as packaging materials, in electronic devices, medical applications, and other consumables (Gilbert, 2017), which our modern society is completely dependent upon. Since 1950 more than 8,300 million metric tons of plastics were produced (Geyer et al., 2017). However, this success also comes at a high environmental cost. An absurd high fraction of these artificial and robust materials accumulates in landfills or in the marine biosphere, where they pollute all kind of lifeforms and sensitive ecosystems. Plastic debris is found even in the most remote locations on Earth such as Antarctica (Waller et al., 2017). At the same time, the high concentration of microplastic in the ocean also poses a health hazard to humankind (Wright and Kelly, 2017). Among other factors, the environmental perspective and the serious threat for world-health initiated a new race for natural alternatives and has led to the discovery of new scaffolds that could replace the all dominant synthetic plastics (Sun, 2005, Satam et al., 2018).

In addition to substitutes to plastic, there is a growing trend to replace other common materials that are essentials of modern life, with materials from natural and renewable sources that could minimize the environmental damage (Varghese and Mittal, 2018). This transition to a circular and biobased economy influences the development of medical applications, construction of buildings, and the fabrics used for clothing, with the result that the demand for new environmentally friendly solutions in every facet of material science is enormous. Another driving force that naturally accelerates the field of material science is the technological development. New technologies require novel materials with specifically tailored nanostructures (Yaghi et al., 2003).

The main focus this thesis will be on the biotechnological aspect of material science. Very popular for modern biotechnological processes, are materials that

are biocompatible, degradable and that can be precisely engineered on a nanoscale. A scaffold that fulfils these requirements are materials that are based on the ordered self-assembly of proteins into nanofibrils. The beauty of protein nanomaterials is that they can be dynamically engineered by introducing modifications in the genetic code, which sets no limits on the creativity. For instance, genetic manipulations can be used to equip protein nanomaterials with hitherto foreign functionalities. Furthermore, proteins are heterologously expressed by microorganisms and do not demand the use of environmentally threating chemicals in any part of their production.

The realization to harness this kind of natural occurring material for purposes other than those intended by nature occurred 18 years ago (MacPhee and Dobson, 2000). In the past 18 years, the field has slowly but steadily gained momentum and has led to a wide range of proof-of-concept materials, but to the best of my knowledge there is no industrial scale or medical implementation yet (Wang et al., 2018).

Superficially, the aim of this thesis is to deliver an important contribution in the quest of developing protein nanomaterials that may one day be used for biotechnological applications. Hence, I identified some key obstacles that need to be conquered before this technology is mature for practical use.

First, I targeted to improve the protocols for assembling the protein nanofibrils (PNF), in order to ensure that the functionality of the active domains displayed on the fibrils is completely retained. Second, I aimed to develop a generic expression platform that is appropriate for upscaling the production of protein nanomaterials. Third, I intended to study materials with high biotechnological relevance beyond the proof-of-concept stage.

Even though protein materials may never replace synthetic plastics themselves, they occupy a niche within biotechnology and biomedicine that cannot be filled with synthetic alternatives. The potential of biobased materials in general, but in particular, protein nanomaterials shall be outlined in this work.

2 Background

2.1 Biobased Materials

Biobased materials are as the name suggests materials that are derived from a biological source, so called biotic materials as for instance wood, cotton, spider silk, *etc*. Biotic materials become biobased materials once they have been engineered or processed, but the term implies nothing with respect to its intended use (Masutani and Kimura, 2015).

In popular media the word 'biomaterial' is often used as a synonym for materials from a biological origin, but this is not appropriate in this case. An accurate definition of 'biomaterial' is 'a substance that has been engineered to take a form which, alone or as part of a complex system, is used to direct, by control of interactions with components of living systems, the course of any therapeutic or diagnostic procedure' (Williams, 2014). Improvement of worldwide healthcare solutions is an ever-pending area that demands innovative biomaterials. In this field, the value of natural polymers for medical applications increases steadily, since they originate from renewable sources and because they are biocompatible as well as biodegradable (Balaji et al., 2018). Applications of carbohydrate-based materials such as chitosan or cellulose include, among others, targeted drug delivery, tissue engineering, and wound healing (Balaji et al., 2018, Mohite and Patil, 2014).

In addition to medical applications, recent research shows that carbohydrates are an interesting scaffold in other areas as well. For instance, nanocellulose fibrils were assembled into macroscale fibers that are far superior over other natural polymers in terms of mechanical durability (Mittal et al., 2018). Furthermore, the combination of carbohydrate fibrils with inorganic nanoparticles, creates several interesting prospects for biotechnology, which have been reviewed in depth by Jebali and co-workers (Jebali et al., 2017).

Biobased materials can also be constructed using programable DNA. Sophisticated DNA sequences can self-assemble by an bottom-up approach at nanometer special resolution to simple junction tiles and to complex 3D structures (Nick McElhinny and Becker, 2014). The same mechanisms can be exploited to assemble DNA based hydrogels and advanced molecular machines. (Li et al., 2018).

2.2 Protein Materials

The ensemble of biobased nanomaterials is not complete, without a discussion of protein-based materials. Proteins are not only, for example, biological signal transducers and nano-sized catalysts, but in addition form the material basis for life. Protein structures, compared to inorganic structures, combine the seemingly incompatible properties strength, robustness and adaptability (Buehler and Yung, 2010). The material properties are encoded within the protein sequence and controlled in most cases by post-translational modifications, auxiliary proteins, and the surrounding chemical conditions. Therefore, protein-based materials are able to cover a broad spectrum of material properties and can be extremely rigid or elastic, dependent on the intended application.

Actin and tubulin filaments are dynamic assemblies and components of the cytoskeleton. The polymerization of the globular proteins is reversible and is dependent upon ATP or GTP hydrolysis. These fibrils are not the strongest biological polymers, since preserving the dynamics, goes along with weaker intramolecular interactions, that consequently leads to a less rigid material (Knowles and Buehler, 2011).

Collagen and elastin are the main components of the extracellular matrix and connective tissues. Bundles of elastin are crosslinked by oxidative deamination of lysines from tropoelastin and confer elasticity to vertebrate tissues. To assemble collagen, the precursor peptide undergoes several post-translational modifications inside the cell before three polypeptide chains form a triple helix known as procollagen. Outside the cell, procollagen is glycosylated and covalently linked to other triple helix strands in order to form the mature fiber.

To orchestrate the assembly of keratin fibrils does not require auxiliary proteins and co-factors. Initially, monomers of type I and type II keratins self-assemble into coiled-coil α-helical heterodimers (Scheibel, 2005), before the dimers align antiparallel into tetramers. The stable tetramers are the building blocks for higher-ordered hierarchical structures. As a result of the rigid structure, keratin is the main constituent of hair, nails, and claws.

The hitherto mentioned protein materials have mainly biological relevance, but are of limited interest from a biotechnological point of view. Still, there are

attempts to design nanoscale transport railways with actin and tubulin filaments (Knoblauch and Peters, 2004) and to invent novel biomaterials using collagen (Cen et al., 2008).

Contrary, spider dragline silk is 'natures high performance polymer' (Whitford, 2005) and was for a long time referred to as the strongest biobased material. This notion has been challenged by the nanocellulose fibers alluded to earlier (Mittal et al., 2018). Still, the potential utilization as a biomaterial, ultra-strong textiles, and as a functionalized scaffold, has triggered a several decade long, world-wide effort in order to understand the material and produce it recombinantly (Jansson et al., 2014, Bittencourt, 2016). To date, Adidas and The North Face have produced prototypes based on spider silk for light weight running shoes and resistant outdoor jackets, respectively (Salehi and Scheibel, 2018).

The spider silk protein-based material relies on the ordered assembly of so called spidroins. Spidroins are 3 - 4,000 long aminoacid residue chains with a distinct N-terminal and a C-terminal domain. Embedded in between these domains are tandem repeats of alternating polyalanine blocks and glycine rich regions. In a spider, the proteins are stored at a concentration of 50% (w/v) in the ampulla. Natural spidroin polymerisation requires gradual extraction of water, and the exchange of Na^+ and Cl^- ions with K^+, H^+, and PO_4^{3-}, which steadily decreases the pH along the spinning duct. Finally, the silk structure can be best described as an arrangement of crystalline antiparallel β-sheet cores, that are connected via unstructured regions. Even though this material has a lot of biotechnological potential, there are still some challenges that need to be overcome. Since the spidroins are extremely long and repetitive proteins, only truncated versions can be produced in *Escherichia coli* (*E. coli*). In addition, the natural silk secretion mechanism has not been completely replicated artificially. Instead, other methods are used for fiber formation, such as wet spinning, electrospinning, and spinning with microfluidic devices (Rising, 2014). A recent breakthrough made it possible to mimic the natural spinning silk conditions, which demand a 50% (w/v) spidroin solution that is subjected to a lower pH to initiate fiber formation (Andersson et al., 2017). However, these *in vitro* produced materials do not yet possess the superior material properties of the natural product (Jannson, 2015, Rising, 2014, Andersson et al., 2017).

Proteins that do not have an innate inclination to form elongated structures can also be utilized for building nanomaterials with specifically tailored functions. These structures include, but are not limited to, artificial protein-based nanocages using DNA-binding-proteins recruited by gold (Ma et al., 2015) or the WA20 dimer, a peptide scaffold for barrels, tetrahedrons, and cubes (Kobayashi et al., 2016). These and similar setups can be used in biosensors,

biomedical applications, as catalytic nanomaterials, and nanowires (Luo et al., 2016).

In general, protein materials are a promising scaffold for supramolecular assemblies that could be used in healthcare, since they can be designed from the bottom-up, due to their inherent self-assembling properties. In addition, protein based materials are biodegradable, and have the ability to mimic native matrix elements (Webber et al., 2015).

The above-named advantages are also true for other types of applications in the biotechnological field. Probably the strongest argument to use peptides/proteins as composites for nanomaterials is the fact that these complex structures are encoded within DNA, which can be easily manipulated and specifically designed on a genetic level. The pre-existing cellular machines *E. coli* and *K. pastoris* make recombinant protein production a routine job, as the route from the manipulated DNA to the correctly folded protein is entirely executed by the microorganisms (Soto, 2014).

2.3 Protein Nanofibrils (Amyloid)

2.3.1 Structure of Protein Nanofibrils

Protein folding is a complex process and its accurate execution is fundamental to enable the correct protein function. The fold is dependent upon the aminoacid sequence and is then governed by the hydrophobic effect, electrostatic interactions, Van der Waals interactions and assisted by intracellular chaperones. The folding pathway guides the unstructured peptide produced by the ribosome towards the native state of the globular protein, which occupies a local minimum on the energy landscape of protein folding (**Figure 1**) (Wei et al., 2017). Therefore, the native fold is only a meta-stable state, or in other words, a cell has to ensure an intact proteome unceasingly by removing misfolded proteins (Chen et al., 2011). If this advanced cellular machinery fails, the ultimate fate of many soluble proteins is the deposition into highly ordered PNF, which is a sinkhole on the energy landscape for protein folds (Adamcik and Mezzenga, 2018, Perczel et al., 2007, Toyama and Weissman, 2011).

Commonly these aggregates are called ‘amyloid’, a name closely associated with medical terminology. The reason is that accumulation of these type of protein aggregates is associated with some of the most devastating neurological and nonneuropathic human diseases. The deposits can occur in vital organs, e.g. the brain, the heart, or kidney and destroy healthy tissue. Among others, the amyloid aggregates cause Alzheimer disease, Parkinson disease, ATTR-

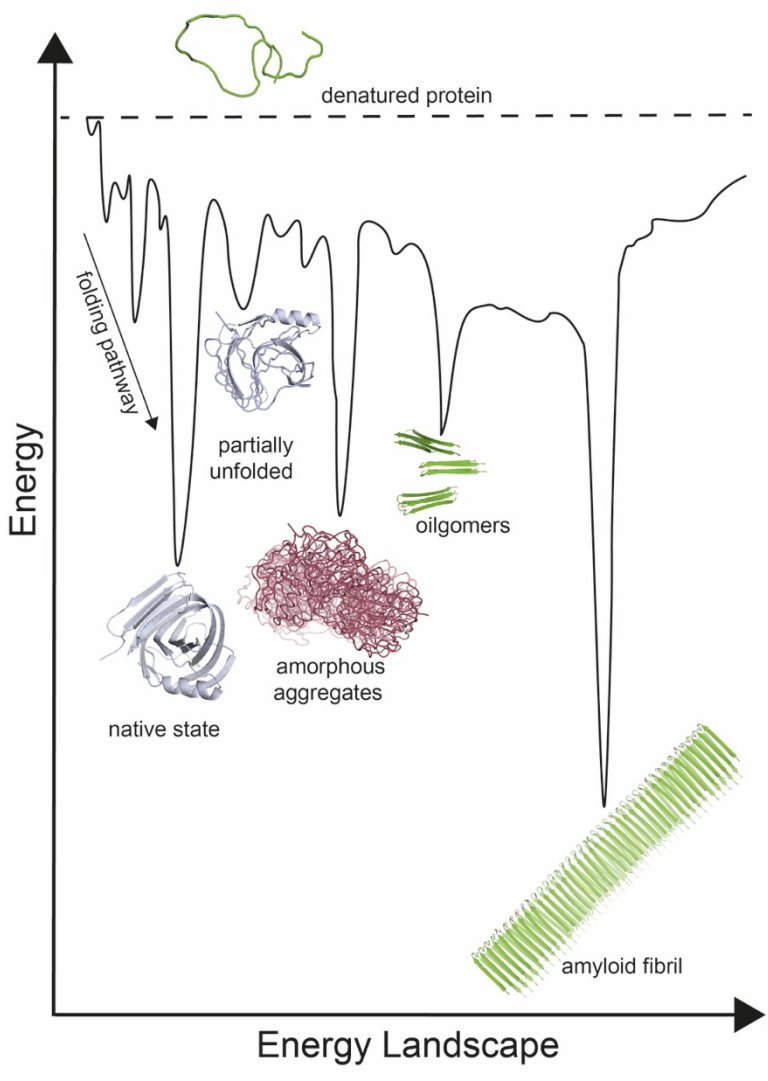

Figure 1. Energy landscape of protein folding (Balchin et al., 2016). The energy levels for the various protein folds is schematically illustrated. The amyloid fold has the lowest possible energy, which explains its stability.

amyloidosis, Huntington's, or type II diabetes (Chiti and Dobson, 2006). Later, I will show that 'amyloid' is not only associated with disease, but that amyloid in many cases is constitutive for physiological functions.

From a structural perspective, the 'misfolded' proteins, are stacked on top of each other to form two or more β-strands, which mainly align in-parallel, and in-register (**Figure 2**) (Luhrs et al., 2005). The β-strands are glued together by

main chain hydrogen bonding. This arrangement leads to long assemblies of β-sheets, which in turn are held together by the hydrophobic effect, side chain hydrogen bonding, or electrostatic interactions (Nelson and Eisenberg, 2006). In the mature fibril, the β-strands are oriented perpendicular to the fiber axis, with the consequence that this configuration is referred to as 'cross-β structure'. The structure in **Figure 2** has been determined with *in vitro* formed aβ42 fibrils, which are normally found in brain deposits of Alzheimer patients. Later studies indicate that the aβ42 aligns as a more complex fibril dimer, but the common characteristics of a cross-β structure still apply (Colvin et al., 2016).

At this point it is important to note that the difference between other protein materials discussed earlier and the amyloid state is that its characteristic architecture is not encoded by a specific amino acid sequence (Schleeger et al., 2013). Instead, the propensity that proteins with, for instance asparagine and glutamine rich regions form amyloid fibrils is higher compared to other regions (Zambrano et al., 2015). In fact, probably most proteins can coalesce into amyloid fibrils if conditions are chosen that promote protein misfolding (Stathopulos et al., 2004, Adamcik and Mezzenga, 2018, Maji et al., 2009, Wei et al., 2017).

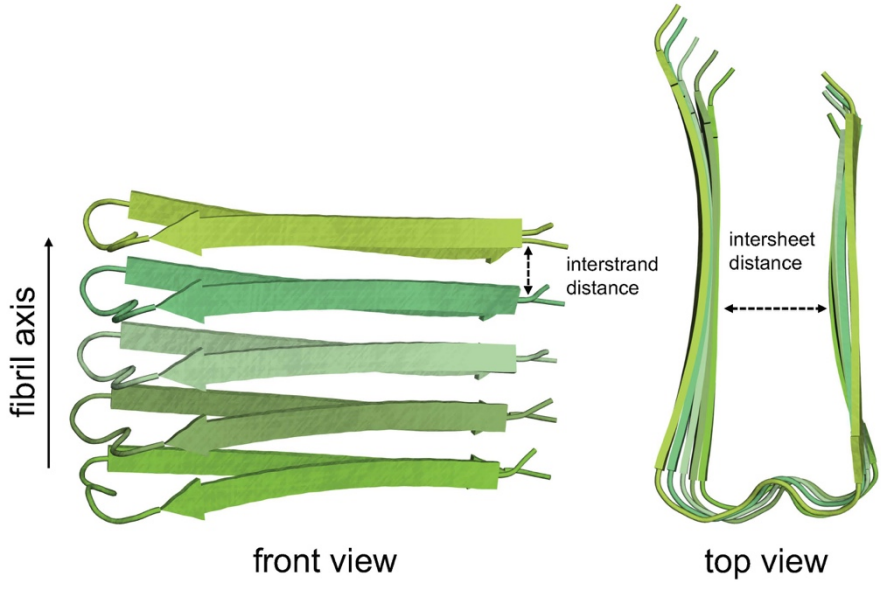

Figure 2. The basic cross-β structure of an aβ42 amyloid nanofibril. During aggregation into nanofibrils the individual peptides refold into one or more β-strands that are stacked on top of each other. The individual peptides are indicated by different shades of green. The interstrand distance is typically 4.7 Å and the intersheet distance is 10 Å. The cartoon structure is derived from the aβ42 structure with the PDB-ID: 2BEG.

2.3.2 Functional Amyloid

The discovery of amyloid that serves an assortment of physiological functions, so-called functional amyloid, is a vivid testament of the fact that this material is more than just the cause of diseases (Li et al., 2014). For instance, *E. coli* secretes curli proteins, which self-assemble extracellularly into curli fibrils and are essential for biofilm formation (Cherny et al., 2005). In the same manner, complex multicellular organisms employ amyloid for specific functions. Lacewings are insects that protect their eggs with silk that shows a cross-β structure (Bauer et al., 2012). Barnacles are marine crustacea organisms that produce underwater adhesive amyloid fibrils, which aids the attachment of the animals to targeted surfaces (Nakano and Kamino, 2015). Another surprising discovery was that the storage of hormones in secretory granules is accomplished through their reversible deposition as amyloid fibrils (Maji et al., 2009).

These and many other findings commenced a paradigm shift from a view that condemned amyloid as a pure pathological entity, to the point that amyloid fibrils are recognized as an excellent material in bio-nanotechnology. To conclude, I want to emphasize the distinction between 'functional' and 'functionalized' amyloid. The very definition of functional amyloid was illustrated in the examples above, *i.e.* amyloid that serves an important physiological role. Contrary, functionalized amyloid are engineered PNFs, by genetic re-design or similar methods, artificially endowed with a foreign functionality.

2.3.3 Material Properties

The incentive that functional amyloid is used for a remarkable collection of diverse application is the advantageous material properties that are exploited by living organisms (Wang et al., 2018, Knowles and Buehler, 2011, Fowler et al., 2007). Amyloid fibrils are self-assembling and possess a high mechanical strength that resembles the properties of spider dragline silk (Knowles et al., 2007, Knowles and Buehler, 2011) (**Table 1**). In addition, the fibrils are chemically and biologically robust. In particular, they can tolerate heating to 100 °C, extreme pH, high concentration of denaturants and salt, as well as proteolytic degradation (Scheibel et al., 2003, Baxa et al., 2004). Dependent on the amyloidogenic peptide the core diameter of the fibrils can be less than 10 nm with a length of several µm (**Figure 3**). Thus, the nanofibrils exhibit an extremely large surface area over volume ratio.

The biotechnological perspective also appreciates, with respect to the material properties, the biocompatibility on account of a minimal immunogenic and inflammatory potential (Hauser et al., 2014). Moreover, fibril modifications that lead to novel functions can be introduced genetically or by other means. Highly amyloidogenic proteins can be truncated, in order to remove domains or regions that are not essential for fibrillation. Additional modifications that can

Table 1. Comparison of the Youngs modulus and the ultimate strength of amyloid with other materials.

Material	Youngs modulus (GPa)	Ultimate strength (GPa)
Diamond [a)]	1000	
Steel [b)]	200	0.6-1.8
Wood [c)]	8-15	
Spider Dragline Silk [d)]	1-10	1-1.5
Amyloid [e)]	0.2-14	0.6
Keratin [f)]	1-3	0.02 - 0.2
Rubber [g)]	0.001-0.01	0.02 - 0.04

The Youngs modulus measures the elastic elongation of the material under stress. The ultimate strength is a measure of the maximal pulling stress necessary to break the material. a) (Savvides and Bell, 1992). b) (Chen et al., 2016). c) (Green, 1999). d) (Vehoff et al., 2007, Agnarsson et al., 2010). e, g) (Smith et al., 2006, Knowles and Buehler, 2011). f) (Bonser, 2000, McKittrick et al., 2012).

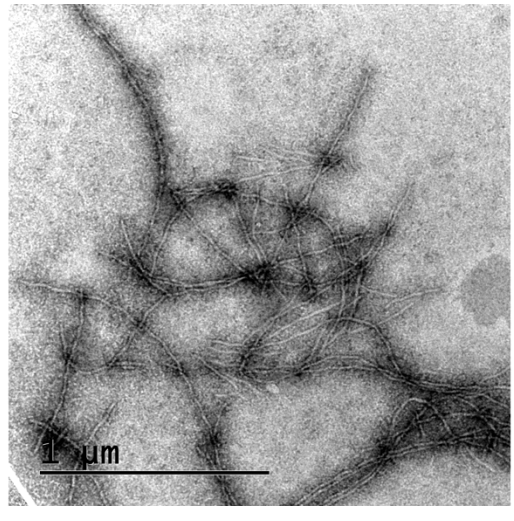

Figure 3. TEM image of amyloid fibrils. Amyloid fibrils can be as short as 100 nm or much longer than 1 µm. The fibril core typically has a diameter of 5-15 nm. The scale bar indicates 1 µm.

be implemented is the re-design of the amyloidogenic peptide sequence and the gene fusion to functional domains. The material is environmentally friendly produced by microorganisms, which means there is no chemistry involved, not even for functionalization. Specific examples of genetic functionalization and other types of modifications that are not introduced through DNA will be discussed later.

Another biotechnological relevant property is that the PNFs can be manufactured into different macro-morphological structures. The most acknowledged examples are threads (Kamada et al., 2017), hydrogels (Loveday et al., 2011), aerogels (Nystrom et al., 2016), foams (Peng et al., 2017), films (Knowles et al., 2010), and beads (Zhou et al., 2015).

Even though functional amyloid is widely used in nature, safety concerns for *in vivo* applications are still prevalent (Wei et al., 2017). Apprehensions are related to potential cross-seeding effects that could cause undesired, pathological protein aggregation *in vivo*. However, the latest research suggests that the mature fibrils are not the cause of toxicity, but instead the fibrillar precursor intermediates (Hauser et al., 2014, Cherny and Gazit, 2008). Still, the safety concerns cannot be completely disregarded. For instance, when a mouse model for AA-amyloidosis was injected with sonicated functional amyloid from *E. coli* and *Saccharomyces cerevisiae* (*S. cerevisiae*), the mouse model showed an early onset of amyloidosis in the spine (Lundmark et al., 2005). At the same time, injection of silk from *Bombyx mori* also resulted in the formation of early amyloidosis in the mouse model. This is not surprising considering that silk is structurally extremely similar to amyloid (Cherny and Gazit, 2008).

2.3.4 Nanofibril Forming Peptides

The scaffold for the design of new protein nanomaterials is an important choice since their properties need to match the application. Factors that might be of importance are the charge of the side chains, the hydrophobicity, the fibrillation kinetics, the peptide solubility, and the peptide size.

There is a broad selection of natural and artificial motifs that are innately prone to immediate aggregation. Among this selection, the fibril forming peptides can be as short as two phenylalanines (Diaz-Caballero et al., 2018, Tamamis et al., 2009). Other artificial peptides such as the β-16 that possesses amphiphilic properties (Kodama et al., 2004), or the β-tail that aggregates very efficiently, were used for functionalization (Hudalla et al., 2014). Natural existing alternatives are curli proteins from *E. coli* (Zhong et al., 2014). The SH3–domain dimer from bovine phosphatidylinositol-3-kinase is a good choice if the application requires that the fibril assembly is restricted, unless a ‘switch’

is activated (Bader et al., 2006). In the case of the $(SH3)_2$, fibrils do not form if the pH is higher than 3. Sometimes, peptides that originate from pathological amyloid are functionalized, for example transthyretin (TTR) (Channon et al., 2008). On account of the still limited understanding of the exact mechanism and risk factors that triggers amyloidosis, these peptides are less appropriate for biotechnological applications.

With this in mind and for our purposes, we decided to employ the intrinsically unstructured regions from Sup35 and Ure2, that natively form functional amyloid in *S. cerevisiae* (Knowles and Buehler, 2011). The reason for this choice was that the two proteins form one of the best characterized functional and functionalized amyloids.

Natively, Sup35 is a translation release factor with 685 aminoacid residues. Fibrillation of Sup35 increases the suppression of nonsense mutations, which means that there is an increased tendency of the ribosome to read through stop codons (DePace et al., 1998). Structurally, Sup35 has three distinct domains. The N-terminal domain (1-114) is rich in polar residues (45% glutamine and asparagine) and tyrosine (18 %) (King, 2001). The M-domain (115-253) has no known function, but is often used to enhance the solubility of the amylogenic N-terminal domain (Glover et al., 1997). The C-terminal domain (254-685) is essential for native functionality. In this work we decided to use a truncated version of Sup35(1-61) as the basis for new PNF, since this fragment has been successfully used earlier *in vivo* and *in vitro* for the same objective (King and Diaz-Avalos, 2004, Men et al., 2009). Sup35(1-61) has a molecular weight of 8,995 kilo Dalton (kDa).

When correctly folded, the ureidosuccinate transporter Ure2 binds and inhibits the protein Gln3, a transcription factor that represses genes involved in metabolizing poor nitrogen sources, when easier accessible sources are present. Hence, the aggregation of Ure2 *in vivo* leads to the uptake of poor nitrogen sources even if easier accessible ones are available (Baxa et al., 2002). The protein has 354 aminoacid residues and possesses two domains. The N-terminal region (1-64) of Ure2 is amyloidogenic and rich in asparagine (42%). Truncated Ure2(1-64) is sufficient for fibrillation but Ure2(1-80) forms fibrils much faster, which is the reason for choosing Ure2(1-80) as an additional scaffold for functionalization (Maddelein and Wickner, 1999, Baxa et al., 2002). Our Ure2(1-80) construct has a molecular weight of 10,793 kDa.

There are no known high-resolution structures of Sup35 or Ure2 fibrils except for the heptapeptide GNNQQNY fragment from Sup35 (Sawaya et al., 2007). However, solid-state NMR experiments have shown that Sup35 nanofibrils have a parallel in-register β-sheet architecture, which agrees with the amyloid structure of the aβ42 peptide (Gorkovskiy et al., 2014). In addition to

the parallel in-register β-sheet structure, electron paramagnetic resonance with Ure2 fibrils suggests a hierarchical organization into a super-pleated β-sheet structure (Ngo et al., 2011).

2.3.5 Applications of Protein Nanofibrils: Current Status

Since the time when amyloids were recognized as a scaffold for self-assembling nanofibrils with prospective applications in biotechnology, numerous ingenious designs of amyloid materials have been developed. To summarize these designs, excellent and comprehensive reviews on functionalized amyloids and applications thereof were recently published (Woolfson and Mahmoud, 2010, Wei et al., 2017, Wang et al., 2018, Knowles and Mezzenga, 2016, Waku and Tanaka, 2017, Hauser et al., 2014, Luo et al., 2016, Díaz-Caballero et al., 2018). Here, I want to provide a concise overview.

Protocols with the aim to create conducting nanowires for potential applications in bio-nanoelectronics are based on the idea to use the PNFs as templates. For instance, after genetically introducing surface cysteines in Sup35 fibrils, conductive nanowires were created by reductive deposition of silver and gold (Scheibel et al., 2003). Instead of metals, nanowires can also be formed with conductive polymers, such as polyaniline. Aniline binds the hydrophobic pockets of amyloid β-sheet rich regions. Thus, polymerisation of aniline to polyaniline by addition of iron(III)chloride in the presence of lysozyme fibrils resulted in a core-shell architecture with good conducting properties (Meier et al., 2015). In a similar fashion, nanowires with metallic organic compounds utilized in OLEDs were assembled (Elfwing et al., 2015). Another alternative is the display of cytochromes on PNFs that natively bind metalloporphyrin (Baldwin et al., 2006).

Enzymatic functionalization of PNFs is a celebrated concept in the literature, since enzyme immobilisation on the fibrils can be attained by genetic engineering, without the use of post-expression crosslinking chemistry. Among the often-cited examples are Sup35 and Ure2 nanofibrils, which were in a proof-of-concept manner functionalized with alkaline-phosphatase, horseradish-peroxidase, barnase, carbonic-anhydrase, and glutathione-s-transferase (Zhou et al., 2014, Baxa et al., 2003, Baxa et al., 2002, Zhou et al., 2015). Alternatively, the immobilisation of enzymes, for instance α-amylase, can also be mediated through a binding domain displayed on *E. coli* amyloid (Nussbaumer et al., 2017).

Certainly, it is also possible to chemically crosslink enzymes to the fibrils after their formation (Raynes et al., 2011). For example, chemical immobilization of enzymes to PNFs was applied to assemble an antibacterial

film. Glucose oxidase, which oxidizes glucose to gluconolactone and reduces O_2 to H_2O_2, was crosslinked to insulin fibrils and embedded in a poly(vinyl alcohol) film (Pilkington et al., 2010). In this setup the accumulation of H_2O_2 acted as an anti-microbial agent against *E. coli*.

Genetic manipulation of amyloid was likewise implemented to endow curli fibrils with underwater adhesive properties (Zhong et al., 2014) and to assemble multicomponent fibrils that display three different fluorescent proteins (Hudalla et al., 2014). The rational design of heptapeptides that form amyloid fibrils resulted in amyloid material that can capture CO_2 and, in a different design, triples the efficiency of retroviral transduction of human cells (Li et al., 2014).

A thrilling development of functionalized amyloid materials is the production of bio-inorganic hybrid materials. For instance, lysozyme fibrils in combination with activated porous carbon acted as water purification filters that could capture toxic heavy metal ions from water solutions (Bolisetty and Mezzenga, 2016). In an effort to exploit the hydrogel forming properties of β-lactoglobulin fibrils with the pH-responsiveness of carbon nanotubes has led to a hybrid material that reversible forms hydrogels (Li and Mezzenga, 2012).

To exploit the biocompatible and biodegradable properties of amyloid, biomaterials are developed that can be used for tissue engineering (Holmes et al., 2000) and targeted drug delivery (Koutsopoulos et al., 2009). Moreover, amyloid fibrils can be valuable to improve diagnostic tools by enhancing the sensitivity of immunoassays (Men et al., 2016).

3 Methodology

3.1 Fibrillation

The most fundamental concept that leads to meaningful research of functionalized PNFs, is a reliable and reproducible method for fibrillation that yields fine dispersed fibrils, when the aggregation has finished. Tuning the fibrillation to the desired outcome, means to reach complete aggregation of the soluble protein, with the result of elongated fibrils that form relatively fast (less than 24 h). This task requires some screening in order to identify optimal fibrillation conditions.

The highly complex aggregation kinetics involve several steps and aggregation species, starting from nuclei, oligomers, to protofibrils, before the mature fibrils are formed. In addition, off-pathway intermediates, such as amorphous aggregates can occur, which adds additional complexity to the reaction. A fibrillation experiment with soluble amyloidogenic proteins in the presence of thioflavin T (Tht), a dye that becomes highly fluorescent at 482 nm (excitation 450 nm) when it binds to β-sheet rich regions, shows a sigmoidal increase of the fluorescence over time. As a consequence, three phases of fibril formation can be distinguished (**Figure 4**) (Arosio et al., 2015). The absence of mature fibrils is distinctive in the beginning of the lag phase, during which no increase of Tht fluorescence is observed. The starting point for fibril elongation in a true monomeric solution, is primary nucleation, a spontaneous event, which is dependent on the monomer concentration and commences on non-fibrillar surfaces (Michaels et al., 2018). As soon as primary nucleation has occurred, the fibril is elongated by monomer addition (Collins et al., 2004). When enough fibril mass has formed, the nucleation event becomes a self-propagating mechanism. The secondary nucleation event is catalyzed by the surface of the amyloid fibril, and is therefore dependent on the total fibril surface area, and the

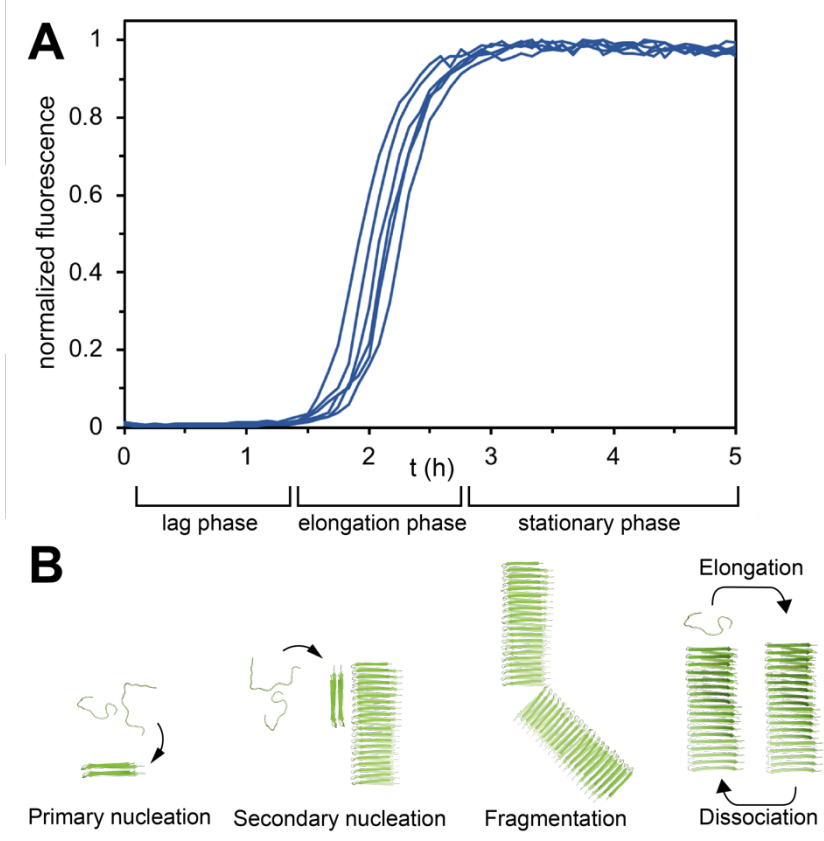

Figure 4. Aggregation kinetics of protein nanofibrils. (A) Together with the dye thioflavin T (Tht), the growth of PNFs from a monomeric sample can be observed using a spectrofluormeter (blue lines, six replicates). The sigmoidal curve shape of fibril formation indicates three phases. During the lag phase the fluorescence is constant at zero. Primary nucleation spontaneously occurs before fibril elongation is initiated. During the elongation phase the Tht fluorescence increases rapidly, due to secondary nucleation events. The increasing fibril surface area serves as a catalyst that promotes the formation of secondary nuclei. As the aggregation progresses, long fibrils are fragmented, which creates new ends for monomer addition. When the monomers are depleted, the reaction reaches the stationary phase, when fibril elongation and dissociation are in equilibrium. (B) Illustration of the different events that occur during fibrillation.

monomer concentration (Meisl et al., 2014). Secondary nucleation accelerates the recruitment of monomers, and is one of the main events during the elongation phase when Tht fluorescence increases rapidly. In addition to secondary nucleation, fibril fragmentation creates additional ends, which makes the consumption of soluble monomers faster, but this event has no influence on the rate of secondary nucleation. Once the monomers of the sample solution are

depleted, the reaction reaches a stationary phase, when fibril elongation thorough monomer addition and dissociation is in equilibrium.

The large number of events that take place during fibril formation, explain the fact that fibrillation can be influenced by several extrinsic chemical and physical factors *in vitro*. Furthermore, the alteration of the conditions does not only influence the aggregation kinetics itself but also the fibril morphology, which is different for each amyloidogenic protein. The single most used factor that controls fibrillation time, is the concentration of the monomer in the sample solution (Hellstrand et al., 2010). Other factors that impact the fibrillation kinetics is seeding (DePace et al., 1998), sonication (Chatani et al., 2009), pH (Giri et al., 2007), temperature (Sabate et al., 2012), salt concentration (Klement et al., 2007, Abelein et al., 2016), agitation (Cohen et al., 2013), or the addition of denaturing agents such as urea or sodium dodecyl sulfate (Khan et al., 2016). By carefully choosing the fibrillation conditions the morphology can be controlled to some degree, but there are no general rules that are valid for all amyloidogenic proteins. Another consideration is that care must be taken if the aim is to assemble, long fibrils, since they will be fragmented by agitation, sonication, and long-time storage (Collins et al., 2004, Ngo et al., 2011).

3.1.1 Fibrillation Methods in the Literature

The complexity of the fibrillation kinetics, and the variety of conditions that can be chosen during fibrillation generate various options to influence fibril formation. Here, I want to focus this discussion on the conditions that have been used in the literature for functionalization of PNFs. Above all, I want to highlight the diversity of fibrillation protocols, with respect to the yeast prion proteins Sup35 and Ure2.

To functionalize PNFs there are two options. The first option is to use chemical conjugation, which is mainly used to create hybrid materials between PNFs and other nanostructures (Wei et al., 2017). The second option is to fibrillate chimeric proteins, or in other words a fusion variant of the protein domain that is prone to assemble into nanofibrils, which will be referred to as the carrier protein, and a functional domain. The functional domain is tethered to the carrier protein *via* a peptide linker through genetic engineering and can be an enzyme or a protein that possesses an affinity for other biomolecules. After expression in the host of choice and purification of the chimeric protein, the protein is fibrillated (**Figure 5**). This strategy to functionalize amyloid fibrils has successfully been used numerous times and does not require the use of chemicals, which is, from an environmental perspective of importance on large

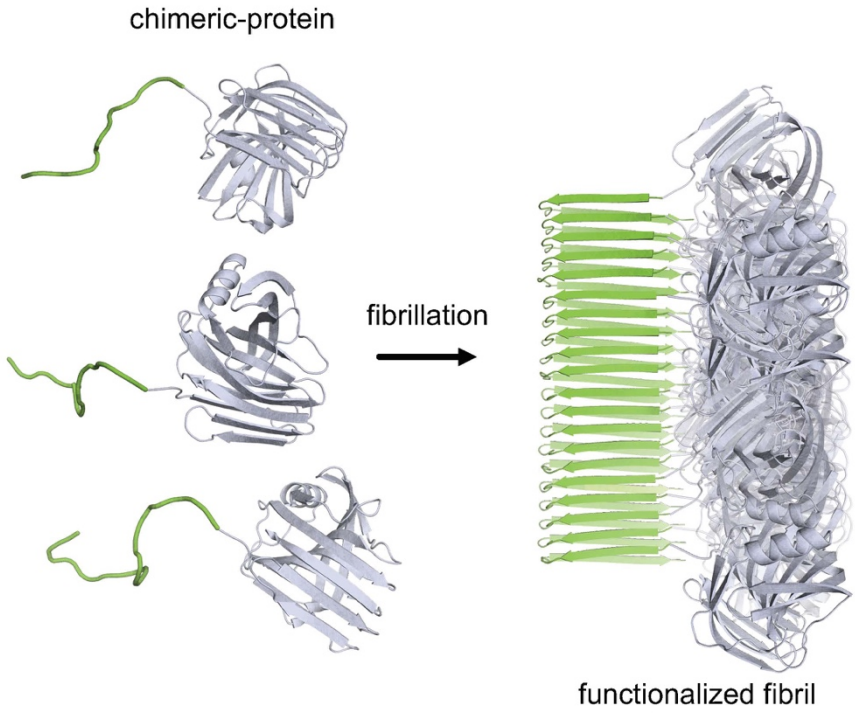

Figure 5. Illustration of the fibrillation of a chimeric protein, a fusion variant of the carrier-peptide (green), which is intrinsically unstructured, and the functional domain (grey). Through fibrillation, functionalized nanofibrils are obtained that display the functional domain on the surface of the fibril. The dense alignment of the functional domain may lead to steric restrictions, on account of the reduced accessibility of the binding pocket or the active site. The figure is a modelled structure using the fibril backbone from aβ42 (PDB code: 2BEG) and the enzyme xylanase A from *Bacillus subtilis* (PDB code: 2Z79).

scales. Another strong suit of this technique is the homogeneity of the immobilized active domains displayed on the PNFs. The functional domain is always linked unidirectionally, either via the N-terminal or the C-terminal end, which ensures an optimal orientation. Contrary to this, traditional enzyme immobilization techniques rely on a heterogenous chemical attachment to the target surface.

At this point it is worth noting that fibrillation using chimeric proteins only (protein fusions of an amyloidogenic carrier with a functional domain), is often accompanied by a reduced functionality. This effect is especially severe for enzymes, and probably originates from the close proximity of one functional domain to the next on the fibril (Wang et al., 2018). Although the peptide linker provides some flexibility, large enzymes are still aligned very tightly, which consequentially limits the accessibility of the substrate to the active site. A

fibrillation strategy that could solve this limitation using a mixture of chimeric proteins and carrier domain proteins will be discussed in the next section.

The conditions to assemble PNFs using chimeric proteins based on Sup35 or Ure2 can differ quite substantially, but is often carried out at physiological pH in a 20 mM NaP_i or tris buffer, containing 200 mM NaCl (Baxa et al., 2011). The temperature for fibrillation can be in range from 4 to 30 °C (Baxa et al., 2011, Zhou et al., 2014, Baxa et al., 2002), either with or without shaking (Zhou et al., 2014, Baxa et al., 2011). To accelerate the fibrillation of chimeric proteins, seeds created by sonication or agitation can be added to monomeric solutions (Men et al., 2010, Scheibel et al., 2003). The time it takes until the fibrils are mature for harvest is method dependent and can vary from 10 minutes to 3 weeks (Men et al., 2010, Baxa et al., 2002). Also, the protein concentration allows flexibility and is typically in the range of 0.1 – 2 mg/ml (Baxa et al., 2002, Baxa et al., 2011). Unfortunately, these studies do not report condition depending data published on the completeness of the fibrillation, *i.e.* the fraction of monomers that were incorporated into the fibril before reaching the stationary phase. However, I can refer to the $(SH3)_2$-Cytochrome C chimera which fibrillates with 70-90% conversion efficiency (Baldwin et al., 2006).

3.1.2 Fibrillation in this Work

On account of the steric restrictions that originate from a too dense packing of the functional domains on the fibril formed by chimeric proteins, we developed a fibrillation protocol that ensures enough accessible space. Instead of fibrillating the chimeric protein alone, we applied a strategy of co-fibrillation. The basis of this strategy is that the chimeric protein is simultaneously fibrillated with the amyloidogenic carrier-protein (**Figure 6**). To initiate the fibrillation a small fraction of the soluble carrier proteins Sup35(1-61) or Ure2(1-80) is briefly sonicated in an ultrasonication bath or with a sonicator for cell lysis, to create fibril seeds. The sonicated carrier proteins are then immediately added to a solution that contains pre-mixed carrier and chimeric protein. Subsequently, the fibrils are allowed to form by over-night incubation at room temperature, in a sterile 1.5 mL Eppendorf vial. To be able to refer to a specific fibril composition independent of the concentrations used during fibrilization we defined the term ‘doping frequency’, which is the molar ratio of carrier protein over chimeric protein.

This strategy yields a fine-tuned nanofibril assembly, where the carrier proteins act as spacers (Paper I and Paper II). Especially functional domains that bind large proteins could benefit from this protocol, as steric restrictions are avoided. Furthermore, enzymes displayed on PNF could completely retain their

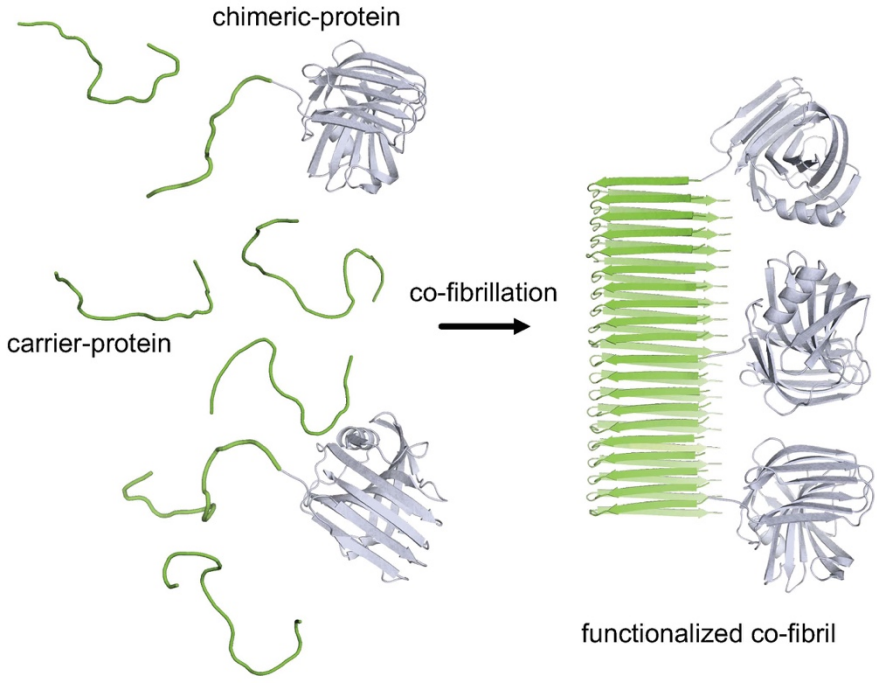

Figure 6. Co-fibrillation of the amyloidogenic carrier proteins (green) and chimeric proteins, a fusion variant of the carrier and the functional domain (grey). The doped nanofibril displays the functional domain on the surface of the fibril. The carrier proteins that are not linked to a functional domain act as spacers to ensure optimal accessibility to the functional domain.

functionality as their active site is not shielded by a neighbouring biocatalyst. We used this functionalization approach in all of our papers (I – IV).

In principle this type of co-fibrillation has been reported in previous studies, but with the perspective to create a fibril array of multiple functionalities. In 2004, Kodama *et al.* reported that fibrillated biotinylated and un-biotinylated peptides were co-fibrillated. The significance of this setup was that the co-fibrillation yielded a regular incorporation of the biotinylated peptide into the mature fibril (Kodama et al., 2004). Another report, published 10 years later, describes the assembly of a multifunctional fibril, which Kodama *et al.* suggested. In this case three fluorescent proteins (green, blue and red fluorescence), were displayed on an amyloid fibril at different ratios. The final fibrillar product possessed a distinct fluorescence that corresponded to the relative amount of each fluorescent protein in the fibril (Hudalla et al., 2014). However, in both instances, the notion that the carrier proteins can be used to ensure accessible space for the functional domains was not considered.

3.2 Fibril Characterization

Once the fibrils were assembled, they were characterized at least with respect to the completeness of fibrillation reaction and their morphology. Certainly, the fibril functionality was also part of the characterization process.

After incubation of the seeded sample containing the carrier and the chimeric proteins the success of the fibrillation was assessed. To this end, the absorbance of the supernatant after centrifugation of the fibril containing sample was carefully measured, to determine the concentration of the non-fibrillated proteins. Alternatively, polyacrylamide gel electrophoresis (SDS- PAGE) was used to compare the protein content of the fibril suspension with the supernatant after centrifugation. This information was of particular importance to be able to calculate the catalytic constants of the enzymes displayed on the protein nanofibrils.

The fibrils were always imaged using transmission electron microscopy (TEM) in order to distinguish between amorphous aggregates and protein nanofibrils. In addition, the TEM images provided morphological information such as fibril length and width.

4 Results and Discussion

4.1 Aims of this Thesis

In general, the aim of this work was to aid the maturation of the functionalized PNF technology. Biotechnological utilization of the PNFs has several challenges, which require optimization of current protocols for fibril assembly and a better understanding of the material. This thesis addresses three of the key construction sites and provides a groundwork for additional efforts to develop PNF technology. In particular, the present studies aimed to:

- Establish a set of applications to stress the versatility of the amyloid scaffold and the concept of a tuned doping frequency in co-fibrillation. The functionalities should be characterized in detail, *i.e.* quantitatively and not only qualitatively.

- Develop a new protocol for PNF assembly that ensures an optimized display of the functional domains on the surface of the fibrils.

- Design a generic microbial protein production method that is scalable and can be used to produce functionalized nanomaterials in a way that requires minimal downstream processing.

4.2 Functionalized Materials Developed in this Work

We were especially attentive to develop PNF materials that are of biotechnological relevance with positive practical implications to problems that await new solutions. A summary of the functional domains tethered to Sup35(1-61) and Ure2(1-80) nanofibrils are found in **Table 2**.

Initially, we functionalized Sup35(1-61) and Ure2(1-80) PNFs with a Z-domain dimer (ZZ) (Paper I and Paper III, **Figure 7**). The Z-domain is an engineered variant of the B-domain, which is part of protein A from *Staphylococcus aureus*. The domain is small (6.6 kDa), has a stable fold, and binds several isoforms of immunoglobulin G (IgG) with an equilibrium dissociation (K_D) in the low nM range. In addition, the Z-domain is also the starting point to create affibody molecules, small alternatives to the 150 kDa antibodies, through *in vitro* directed evolution. By displaying ZZ on the PNFs we sought to exploit the large surface area over volume ratio of the PNFs. The objective was to create an antibody binding nanofibril, with a high IgG binding capacity that could compete with other affinity matrices, such as protein A Sepharose (GE Healthcare).

Contrary to Paper I & III, we focused on the concept of enzyme immobilization in Paper II & IV. Immobilizing enzymes on PNFs has been done several times before, and it is not more complicated than genetic fusion of the carrier protein to the functional domain. To make things even simpler the complete gene can be purchased directly and ligated into the vector of choice, before it is expressed in *E. coli* and purified by chromatographic methods.

With respect to enzymes the biggest restraint is to find suitable candidates. In principle all enzymes can be excluded, except those that are active as a monomer. Many enzymes are dimers or possess even more complicated tertiary structures, which makes the production of chimeric proteins difficult. If no alternatives exist, genetic dimer fusions may mimic a monomer, but the construction of such an ensemble could be time consuming. Other properties that need to be considered when choosing enzymes for PNF functionalization is the long-term stability, availability of co-factors, and any requirement for auxiliary proteins. For our purposes we also preferred that the functional entities are soluble and expressible in *E. coli*.

Table 2. Functionalized materials demonstrated in this work.

Fusion protein	Application	Paper
Z-domain dimer	Antibody purification and immunoassay	I & III
β-Lactamase	Penicillin degradation	II
Carbohydrate processing enzymes	Processing biomass	IV

In Paper II we immobilized the β-Lactamase TEM1 from *E. coli* on Ure2(1-80) fibrils (**Figure 7**). The enzyme hydrolyzes β-lactam antibiotics such as penicillin and ampicillin and could be a valuable tool to ensure that antibiotics are not released into the environment. We specifically chose to study the kinetics of this enzyme because it has a k_{cat}/K_M that is close to the limit of diffusion.

In Paper IV, we advanced the concept of enzyme functionalization one step further and designed an entire reaction cascade build from three enzymes (**Figure 7**). We combined xylanase A (XynA) from *Bacillus subtilis* (Bourgois et al., 2007), β-xylosidase (βXyl) from *Caulobacter crescentus (Correa et al., 2012)*, and an pyrroloquinoline quinone dependent aldose sugar dehydrogenase (ASD) from *E. coli* (Southall et al., 2006) to hydrolyse and oxidize the polysaccharide xylan into xylonolactone.

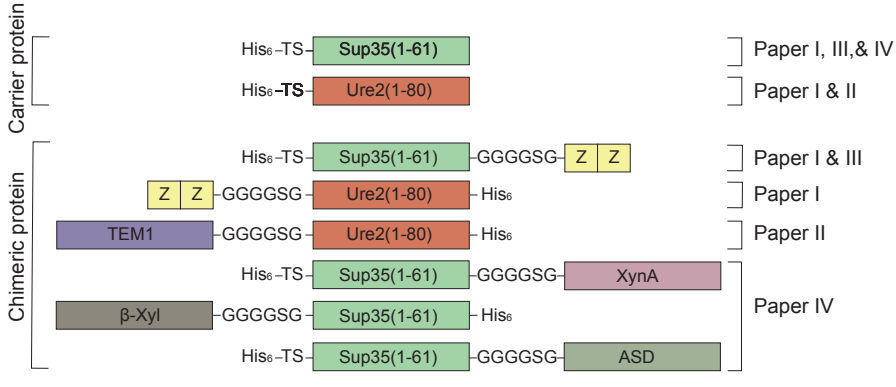

Figure 7. Protein constructs in this work. The histidine tag (His_6) was used for protein purification. The abbreviation TS refers to a thrombin cleavage site. To link the carrier and the functional domain a GGGGSG peptide was used.

4.3 Sup35(1-61) and Ure2(1-80)

The truncated carrier proteins Sup35(1-61) and Ure2(1-80) were expressed in *E. coli*, but accumulated as insoluble inclusion bodies during cultivation. Therefore, we used 8 M urea, to solubilize the inclusion bodies and subsequently purified the proteins with immobilized metal ion affinity chromatography (IMAC) followed by ion exchange chromatography (IEX). The production yield of a 1 L *E. coli* culture varied for both proteins from batch to batch, but was in the range of 5-20 mg/l after IMAC purification. The two carrier proteins had to be flash frozen and stored in 8 M urea at -80 °C, and were stable for at least one year after purification. Higher temperatures (-20 °C) were not appropriate for storage, since aggregates formed immediately when the protein solution was thawed. We were also careful to reduce the sample handling time at room temperature as much as possible. Matrix assisted laser desorption ionization-time of flight mass spectrometry (MALDI-TOF MS) experiments have shown that almost one half of Sup35 is carbamylated already after 48 h in 8 M urea (**Figure 8**).

The lag time for Ure2(1-80) (5 μM) and Sup35(1-61) (5 μM) at 37 °C (100 rpm) is on average 5.7 h and 13.8 h, respectively, which implies that Ure2(1-80)

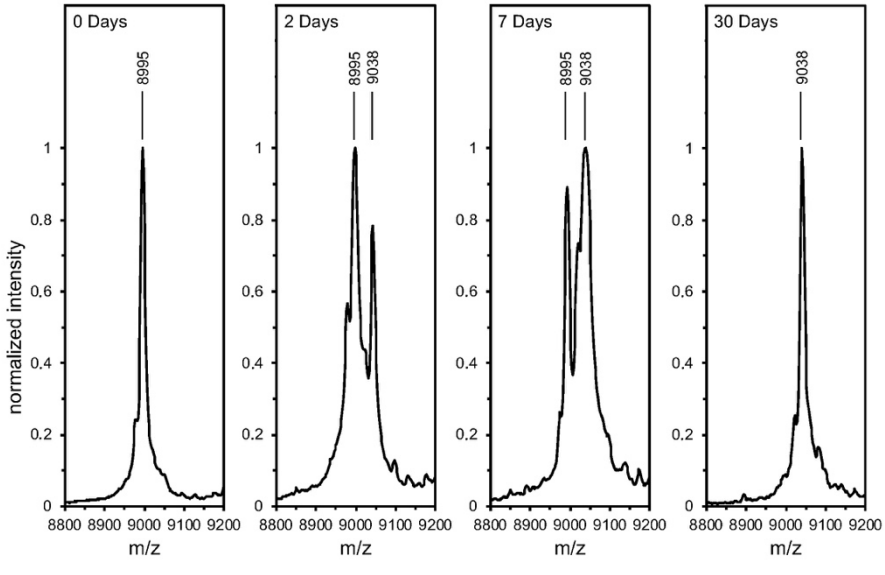

Figure 8. MALDI-TOF MS of Sup35(1-61) stored in 8M urea for 0, 2, 7, and 30 days. In the beginning of the storage the protein has a mass of 8995 Da, but during storage the N-terminal end is carbamylated and gains 43 Da. After 30 days of storage, all protein is carbamylated.

fibrillates faster (**Figure 9A**).[1, 2] Using identical conditions, we also co-fibrillated 5 µM Sup35(1-61) with 0.25-5 µM Sup35(1-61)-ZZ (**Figure 9B**). Addition of the chimeric protein to the carrier protein shortened the lag time by a factor of three. On the contrary, the lag time was either not influenced or extended when 5 µM Ure2(1-80) was co-fibrillated with TEM1-Ure2(1-80) in the range of 0.02-0.5 µM (**Figure 9C**). Even if the effect is more severe for Ure2(1-80), the common denominator in both setups is that higher concentration of chimeric protein renders a lower fluorescence amplitude in the stationary

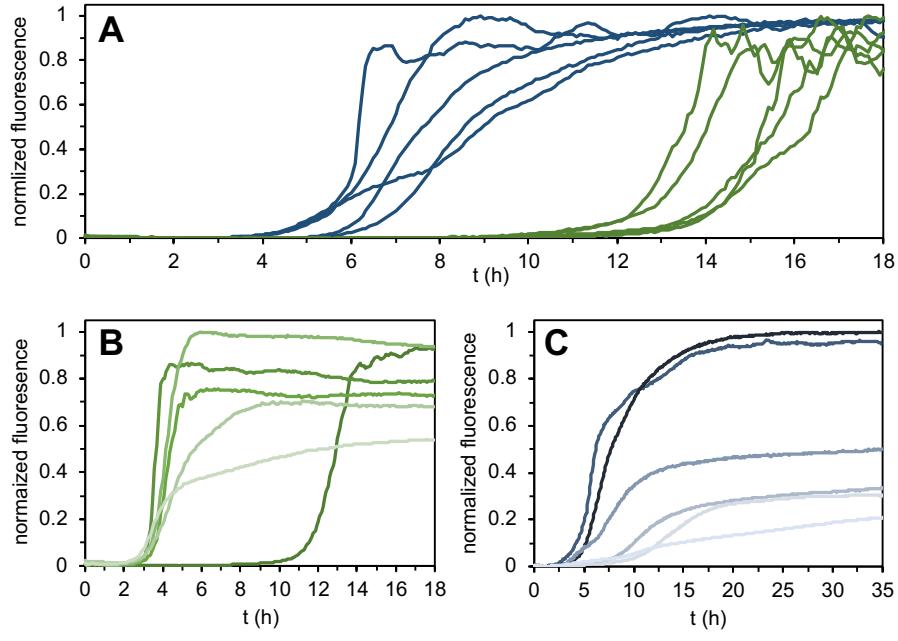

Figure 9. Tht fibrillation assay. (A) Fibrillation of 5 µM Ure2(1-80) (blue) and 5 µM Sup35(1-61) (green) at 37 °C and 100 rpm in quintuplicates. (B) The same conditions as in (A) but in this case 0, 0.25, 0.5, 1, 2.5, or 5 µM Sup35(1-61)-ZZ (in the same order dark to light-green) was added to 5 µM Sup35(1-61). (C) The same conditions as in (A). Here, 5 µM Ure2(1-80) were fibrillated together with 0, 0.02, 0.05, 0.1, 0.2, and 0.5 µM TEM-Ure2(1-80) (in the same order dark to light-blue). The fibrillation curves in (B) and (C) are averages of six replicate experiments. The data shown here is not published.

1. This is only valid for a black 96 well Nunc X180 Microplate (Polystyrene, Thermo Scientific) covered with Nunc X100 sealing tape (Thermo Scientific). The sample volume was 100 µl in a 10 mM KP_i buffer containing 150 mM NaCl, 50 µM ThT, at pH 7.4.

2. It is not possible to compare these values with already published data to draw conclusions for two reasons. (1) Most reports discuss fibrillation of Sup35(1-254). (2) There is no standard protocol in the preparation and fibrillation of Sup35, as it is the case for aβ42.

phase. This indicates that only a fraction of the carrier and chimeric proteins are fibrillated.

Recovery of the fibrils formed in the 96-well plates proved to be extremely difficult since they were inseparable from the polystyrene surface. Since the ultimate aim was not to study the fibrillation kinetics, but to assemble doped nanofibrils for enzyme and binding kinetic characterizations, we moved from the 96-well plate to Eppendorf tubes (polyethylene). The results from our initial co-fibrillation experiments suggested that it is difficult to co-fibrillate using higher amounts of chimeric proteins. Therefore, we developed a new fibrillation protocol that would yield complete fibrillation of both the carrier and chimeric proteins. The best results with respect to complete fibrillation were achieved when a small portion of soluble carrier protein was sonicated to create seeds. After sonication the seeds were added immediately to an Eppendorf vial, containing pre-mixed chimeric and carrier protein. The mature functionalized fibrils formed during overnight incubation.[3]

Another essential characteristic of the carrier proteins, which we verified was whether or not they restrain the functional domain of a chimeric construct. To elucidate this inquiry, the binding rates for the Z-domain dimer linked to Ure2(1-80) and Sup35(1-61) was determined with a surface plasmon resonance (SPR)-assay (**Table 3**). As a reference served the Z-domain without a tag, with the result that the carrier protein has no effect on ZZ. Likewise, the functionality of the enzyme-carrier protein chimeras was characterized by determination of the Michaelis-Menten constants (k_{cat} and K_M) and compared to literature values, where available. In the same way we concluded that the carrier protein tag has no effect on the activity of linked enzymes, at least in the case of TEM1 and βXyl.

We think that the discrepancy between the k_{cat} values of ASD is not due to enzyme inhibition by the Sup35 tag, but rather due to calculation errors in the reference paper (Southall et al., 2006). The enzyme assay is based upon the oxidation of xylose to xylonolactone in the presence of 2,6-dichloroindophenol (DCIP), which is simultaneously reduced ($\Delta\varepsilon_{600} = 21\ mM^{-1}\ cm^{-1}$). According to the materials and methods section the enzyme assay was executed as follows: The reduction of 50 µM DCIP was recorded for 150 s with a spectrophotometer, in the presence of 100 mM glucose and 1-8 µg enzyme, in a 1 mL cuvette. From Figure 3 in the reference paper we know that the enzyme activity was at least 400 U at pH 8.75, were 1 U is defined as 1 µmol/(min mg). Thus, in this specific assay, 5 µg enzyme (from Figure 3 in the reference paper) should be able to oxidize glucose, and likewise reduce DCIP, at a rate of 2 µmol/min. Considering that DCIP amount in the cuvette was 50 nmol, the dye would have been

3. Experimental data is found in the Supporting Information of Paper I and Paper II

Table 3. Binding and catalytic constants of Sup35(1-61) and Ure2(1-80) tagged functional proteins are compared with reference values.

soluble chimeric protein	k_{on} ($M^{-1}s^{-1}$ x 10^5)	k_{off} (s^{-1} x 10^{-4})
Sup35-ZZ[a]	3.8 / 2.4	1.0 / 3.4
ZZ-Ure2[a]	4.2 / 2.4	0.7 / 3.4

soluble chimeric protein	k_{cat} (s^{-1})	K_M (μM)
TEM1-Ure2[b]	1396 / 1428	41 / 50
βXyl-S35[c]	21 / n. a.	7.4 / 9.3
Sup35-ASD[d]	5 / 3360	$382*10^3$ / $400*10^3$

The experimental values are compared to reference values in the format 'experimental / reference'. a) Experimentally determined binding constants to IgG are compared to binding constants for the untagged Z-domain (Paper I). b) Experimentally determined catalytic constants (Paper II) are compared to literature values using the substrate ampicillin. c) The catalytic constants are reported in Paper IV. No reference value for k_{cat} for this particular enzyme was reported in the literature (substrate: pNP-X). d) Experimentally determined catalytic constants from Paper IV with xylose as the substrate. The K_M value are comparable to values from the literature but k_{cat} (glucose) is apparently 1,000-fold reduced. An explanation can be found in the text.

consumed within 1.5 seconds, which makes it impossible to follow the reaction for 150 s, as stated in the material and methods section. Obviously, the authors made some serious errors in their activity measurements, which undermines the credibility of the reported k_{cat} value. Unfortunately, we were not able to find other reports for the catalytic efficiency of ASD from *E. coli* in the literature. However, another monomeric ASD from the thermophilic organism *Pyrobaculum aerophilum* has a k_{cat} of 3.2 s^{-1} (Sakuraba et al., 2010), which agrees well with the k_{cat} value determined in Paper IV.

4.4 The Concept of Doped Nanofibrils

In several works that functionalize nanofibrils by genetically and chemically linking enzymes to the amyloidogenic carrier proteins (see **Figure 5**) a severe reduction of the catalytic efficiency is observed (Baxa et al., 2002, Zhou et al., 2014, Wang et al., 2018, Pilkington et al., 2010, Raynes et al., 2011). We speculated that the proximity of one functional domain to the next is the main factor that contributes to this effect, as dense packing could lead to shielding of the active site/binding site of a functional domain. The main objective of Paper I was to elucidate whether or not this hypothesis is true. In Paper II we sought to

confirm that the functionality of TEM1 with a catalytic efficiency near the limit of diffusion is completely retained when it is displayed according to our functionalisation-hypothesis. Even if this hypothesis is not discussed in Paper III and IV, fibrillation to assemble functionalized fibrils was carried out according to the same protocols.

In Paper I we decorated Sup35(1-61) and Ure2(1-80) nanofibrils with the Z-domain dimer by simultaneous fibrillation (see the concept in **Figure 6**) of the carrier protein and the chimeric proteins (**Figure 7**). The Z-domain dimer was an ideal candidate for the purpose of testing the functionalization-hypothesis as it is a small domain that binds IgG, which is 15 times larger. An optimal point for functionalization should become evident by determination of the IgG binding capacity as a function of the doping frequency. Therefore, we assembled a set of fibrils with a doping frequency between 1:0.04 and 1:0.65 for Sup35(1-61) and in the range of 1:0.04 to 1:0.9 for Ure2(1-80) fibrils. The binding capacity of human IgG for each fibril was determined in six experimental replicates. In this experiment, we found evidence that supports our hypothesis, since we demonstrated that both fibril scaffolds have indeed an optimal ratio of carrier over chimeric protein. The best doping frequency was 1:0.33 (binding capacity 1.8 mg IgG /mg fibril) and 1:0.49 (binding capacity 1.7 mg/mg), for Sup35(1-61) and Ure2(1-80) fibrils, respectively (**Figure 10A, D**). A higher doping frequency above these points reduced the functionality significantly (**Figure 10C, F**). For instance, IgG occupies 60% of all possible Z-domain dimer binding sites in a 1:0.33 Sup35-fibril but only 40% if the doping frequency is 1:0.65. The same relationship is also true for Ure2 fibrils. Furthermore, it is interesting to note that our data confirms that the IgG molecules require a minimum amount of space along the fibril. The antibodies claim on average 6.5 fibrillated Sup35(1-61) proteins and 5.8 Ure2(1-80) proteins (**Figure 10D, E**), which corresponds to 3-3.5 nm fibril length (**Figure 2**). This number is constant for doping frequencies above 1:0.49 and indicates that an even tighter arrangement of antibodies is not possible. Thus, any additional ZZ-domains are inaccessible and lower the binding capacity.

Inspired by these findings, we verified if the catalytic efficiency of TEM1 on Ure2 fibrils is reduced by steric restrictions if we equip the fibrils with a low enzyme density (Paper II). First, we determined the k_{cat} and K_M of fibrils with a doping frequency in the range of $1:1*10^{-3}$ to $1:30*10^{-3}$. These initial results showed a severe reduction of k_{cat} by a factor of 10 compared to the soluble protein. The reduction of k_{cat} was independent of the doping frequency. Contrary to this observation, the K_M is linearly increased with the doping frequency, which indicates mass transport limitation. Therefore, to determine the actual maximal turnover rate we mounted the fibrils in a flow reactor, to be able to deliver the

substrate to the enzyme by flow and not by diffusion. In this setup we determined that the maximal rate of hydrolysis of TEM1 immobilized on the PNFs is 1122 s^{-1}, which corresponds to 80% of the soluble enzyme (**Table 3**). In conclusion, these results serve as a further evidence that supports our functionalization-hypothesis.

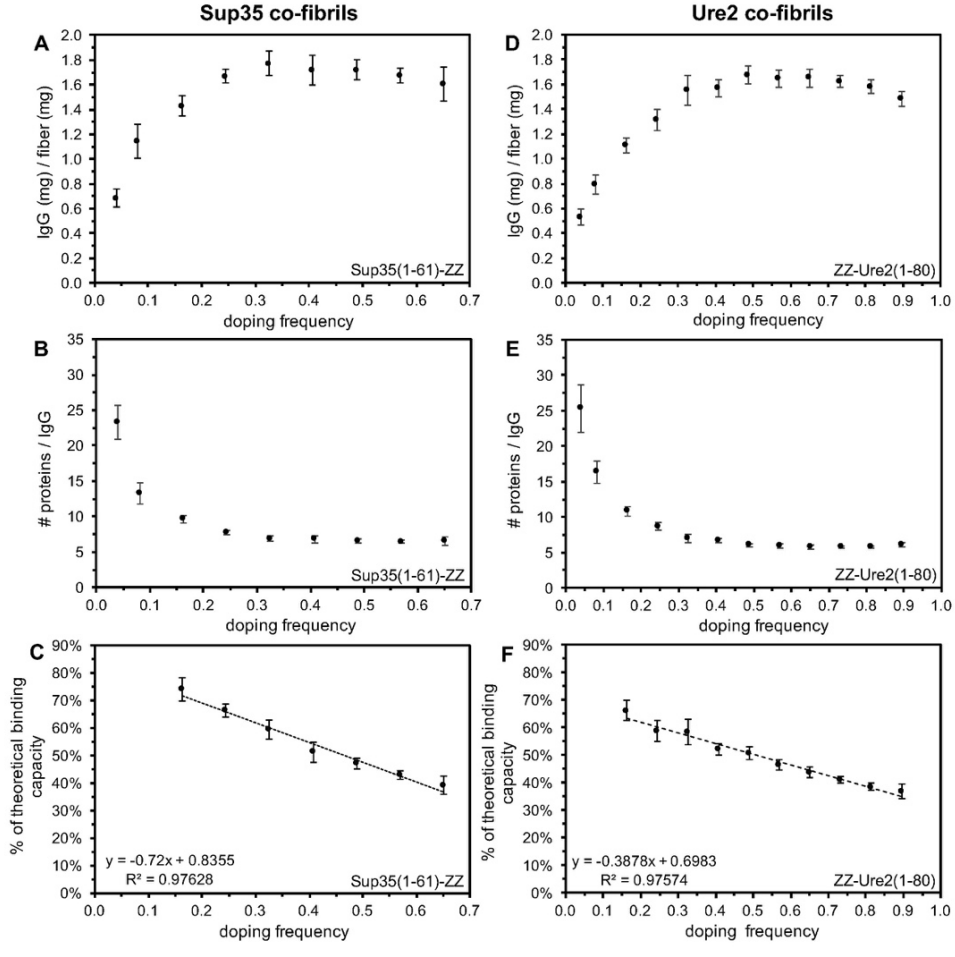

Figure 10. Optimized doping frequency of Sup35(1-61) and Ure2(1-80) nanofibrils (Paper I). The left-hand panel shows data for Sup35 fibrils and the right hand-panel refers to Ure2 fibrils. (A & D) The IgG binding capacity of ZZ-domain doped nanofibrils is plotted as a function of doping frequency (molar ratio of carrier over chimeric protein). (B & E) The number of fibrillated monomers that are necessary to bind one antibody. (C & F) Linear dependency of the theoretical binding capacity (assuming that all ZZ-dimers bind one molecule IgG) as a function of the ZZ-domain doping frequency. The figure was reproduced with the permission from the publisher.

4.5 Enzyme Kinetics of Functionalized Nanofibrils

4.5.1 Kinetic Model for Enzymatically Endowed Nanofibrils Trapped in a Column

So far, reports of enzymatic functionalisation of PNF in the literature have been limited to a qualitative level. New functional endowments are presented in a proof-of-concept manner, where k_{cat} as well as K_M of the fibrils are reported, but additional kinetic characterizations are missing (Zhou et al., 2014). In addition, speculations that mass transport, steric restrictions or both are the cause for a severe reduction of enzymatic efficiency have not been further investigated. Nevertheless, an answer to this issue is constitutive, for the development of biotechnological applications. Therefore, in order to go beyond the simple qualitative stage, we trapped Ure2 fibrils that display TEM1 in a microcolumn (Paper II). In this setup, fibrils with a doping frequency of $1{:}3*10^{-3}$, $1{:}6*10^{-3}$, $1{:}12*10^{-3}$, and $1{:}30*10^{-3}$ were embedded between two 0.45 µm filters. The filters were important to avoid premature contact of the enzyme with the substrate solution containing ampicillin, which was forced through the column by centrifugation. The amount of hydrolysed ampicillin after passing through the layer of TEM1 functionalized fibrils was determined by measuring the absorbance at 235 nm ($\Delta\varepsilon_{235}$ = 900 M^{-1} cm^{-1}). Together with the flow rate, we were able to calculate the number of hydrolysed substrate molecules per enzyme each second as

$$\frac{\Delta[S]Q}{E_{tot}} \tag{1.}$$

where Q is the flow rate $V/\Delta t$, E_{tot} the total enzyme amount (mol), and $\Delta[S]$ the difference of the substrate concentration after fibril passage. This expression was related to the total number of available substrate molecules per enzyme each second. To explain the data, we re-derived the Michaelis-Menten equation with the assumption that the flow, rather than diffusion transports the substrate to the enzyme. Here, we obtained an equation that resembles the Michaelis-Menten equation

$$r_0 = k_2\left(\frac{\frac{[S]}{[E]_{tot}}\frac{Q}{V_R}}{\frac{[S]}{[E]_{tot}}\frac{Q}{V_R}+K_{M,flow}}\right) \tag{2.}$$

where r_0 is the rate of product formation per enzyme, k_2 the maximal substrate turnover rate, $[E]_{tot}$ the total enzyme concentration in the reaction volume V_R. $K_{M,flow}$ can be interpreted as the number of substrate molecules available per enzyme each second in order to reach ½ k_2. Since the reaction volume (the volume of the fibril layer) cannot be easily determined, we multiplied $[E]_{tot}$ with V_R, which yields

$$\frac{[S]}{[E]_{tot}} \frac{Q}{V_R} = \frac{[S]Q}{E_{tot}} \qquad (3.)$$

Classically, the Lilly-Hornby equation is used for the purpose of characterizing an immobilized enzyme, in a flow reactor (Urban et al., 2006). To be able to fit the enzyme kinetic data to the Lilly-Hornby equation, the converted substrate amount after column passage is determined for four (or more) flow rates, as a function of substrate concentration (Seong et al., 2003). The model yields two parameters. The reactor capacity C is only valid for the specific enzyme amount immobilized in the flow reactor and is reported for all flow rates. The same applies to the (apparent) substrate concentration $K_{M(app)}$ when the biocatalyst reaches half of the maximal turnover rate.

Since centrifugation of our microcolumn was not able to yield an identical substrate flow rate every time, we had to choose an unconventional approach and plotted our data as $\Delta[S]QE_{tot}^{-1}$ over $[S]QE_{tot}^{-1}$. Altogether, 35 measurements of the catalytic fibrils with four different TEM1 doping frequencies merged into a hyperbolic curve (**Figure 11**). The data was fitted to equation (2.) with the result that the maximal turnover rate of TEM1 displayed on Ure2(1-80) is 1122 s^{-1}. Notably, the rate constant is indeed almost identical to the k_{cat} of the soluble enzyme. Therefore, the origin of the reduced catalytic efficiency of the TEM1 functionalized fibrils in suspension can only be explained by mass transport limitations and not steric restrictions.

To validate our model further, we tested if equation (2.) can be used to fit data from previous publications that relied on the Lilly-Hornby equation. To this end, we converted the data from several articles to $\Delta[S]QE_{tot}^{-1}$ over $[S]QE_{tot}^{-1}$. In **Figure 12** we have chosen to include a representative collection which includes data from the original paper published by Lilly and Hornby (**Figure 12C & D**) and other more recent studies (**Figure 12A & B**) (Lilly et al., 1966, Mansfeld and Schellenberger, 1987, Matosevic et al., 2011). **Figure 12A & B** strongly indicate that equation (2.) is not only valid for the TEM1-Ure2(1-80) fibril reactor, but generally applicable. Moreover, the data plotted in **Figure 12C & D** fits rather poorly to equation (2.), but the overall trend still suggests a hyperbolic dependency. In conclusion, instead of reporting the column capacity C and an

apparent $K_{M(app)}$, which has limited meaning for comparison purposes, our new model makes catalytic columns extremely comparable. Equation (2) yields two constants, k_2 and $K_{M,flow}$ that are independent on flow rate and enzyme concentration. These constants can be used in the same way as k_{cat} and K_M are used to characterize enzymes.

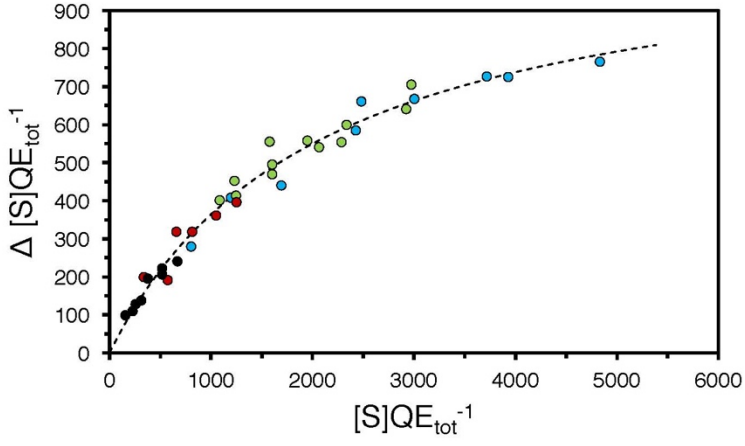

Figure 11. The number of substrate molecules hydrolysed by each enzyme each second as a function of the total number of substrate molecules that encounter each enzyme each second. The hydrolytic events were measured with TEM1 functionalized fibrils with doping frequencies of $1:3*10^{-3}$ (blue), $1:6*10^{-3}$ (green), $1:12*10^{-3}$ (red), and $1:30*10^{-3}$ (black), trapped in a microcolumn. This data was fitted to equation (2., dashed line), which yielded the constants k_2 (maximal substrate turnover rate) and $K_{M,\,flow}$ ($[S]QE_{tot}^{-1}$ at ½ k_2).

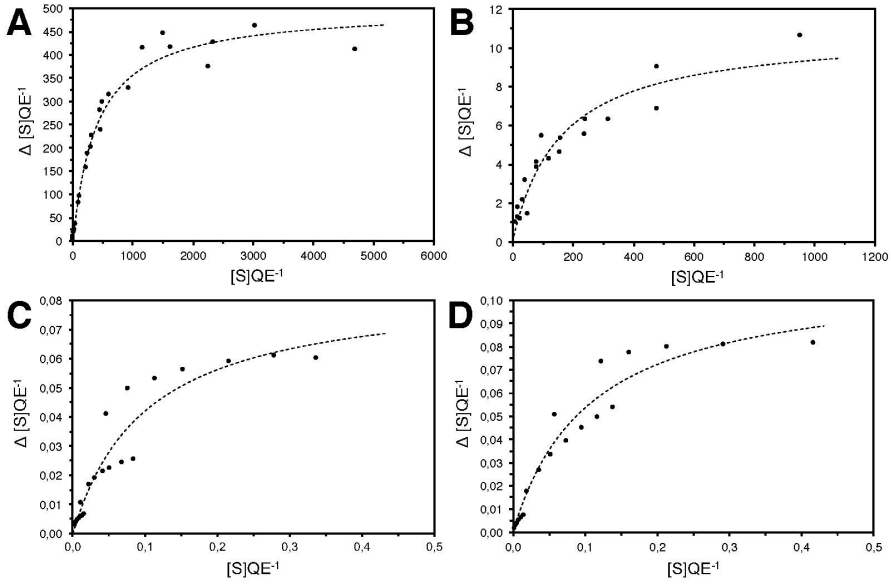

Figure 12. A-D Examples of data from the literature converted to $\Delta[S]QE_{tot}^{-1}$ over $[S]QE_{tot}^{-1}$ and fitted to equation (2.).

4.5.2 A Cascade Reaction Catalysed by Three Enzymes Immobilized on Nanofibrils

Enzyme immobilization using amyloid fibrils is a well-established method, which was already demonstrated using several different biocatalysts (see section 4.4). Although this kind of functionalized fibrils are relatively easy to assemble, only one example of a two-enzyme cascade was discussed in the literature (Nussbaumer et al., 2017). Since enzymatic cascade reactions could be used for the cell-free synthesis of commodity chemicals, the potential that amyloid fibrils hold in this respect have not been investigated to its fulness. Paper IV is an important step towards this aim. Here, a three enzymatic cascade (XynA, βXyl, ASD) that converts xylan from beechwood to xylonolactone was studied, which includes a detailed kinetic analysis of the factors that influence product accumulation.

Our initial idea was to create a modular cascade of functionalized PNFs that are separately captured on 0.45 µm filters (**Figure 13**), similar to a previously suggested concept for spider dragline silk (Jansson et al., 2015). In this design, the substrate solution is cycled over the filters until the desired product

concentration is reached. The advantage is that possible mass transport limitations are counteracted by increasing the flow of the substrate solution. Suspecting that the filters could be clogged by an improper preparation of the beechwood xylan, we were very careful and filtered the substrate solution several times through 0.2 µm. Also, an initial test of cycling the substrate over empty 0.45 µm filters maintained a stable pressure for 24h. However, once the fibrils were placed on the filter, the back pressure increased steadily to sustain a reasonable flow rate of 0.5 mL/min, until the filter was completely clogged. A plausible explanation is that the initial rather loose packing of the fibrils is crushed by the back pressure, which means that flow channels cease to exist. To omit these complications, we decided to study a fibril suspension instead.

The primary investigation focused on the synergy between XynA and βXyl, which liberates xylose monomers from beechwood xylan. This catalytic reaction was strategically studied by first determining the relative molar ratios of the soluble enzymes that yield the highest xylose concentration after a 24 h incubation at 37 °C. At 0.4 µM XynA, the xylooligos (xylobiose, xylotriose, xylotetraose, xylopentaose) reach their highest concentration during the first 240 minutes (pH 6). From this point on, their concentration is steadily decreased, and xylose concentration is increased, due to the action of βXyl. A 30-molar excess

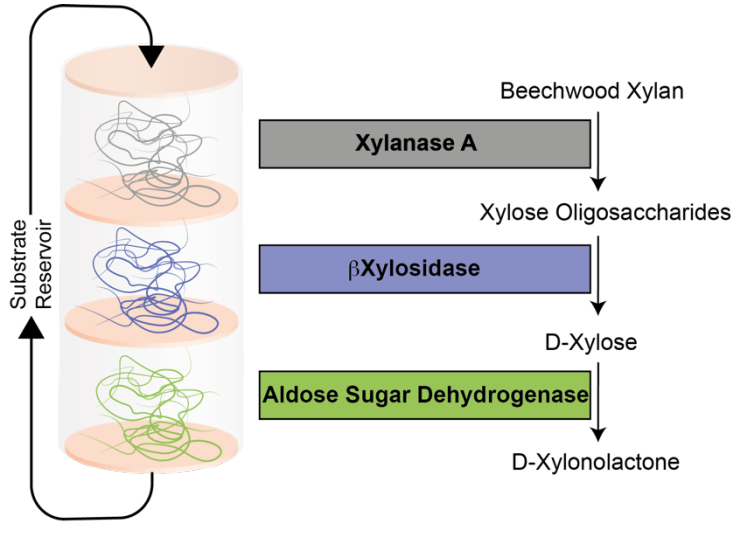

Figure 13. The initial concept for implementing the enzymatic cascade includes the enzymes XynA, βXyl and ASD immobilized on PNF. These enzymes convert long chained carbohydrates (xylan) to xylonolactone. The design relies on capturing the fibrils on 0.45 µm filters, which allows substrate cycling over the filter until the desired product concentration is reached. By adjusting the flow rate, mass transport limitations could also be decreased.

βXyl over XynA yielded 64% xylose with respect to the total product concentration.

This reaction was replicated, but this time the enzymes were displayed on Sup35 fibrils (doping frequency 1:0.74 and 1:0.33 for XynA and βXyl fibrils, respectively). In fact, this comparison revealed no difference between the product yield and the relative xylooligo content, which yet again points towards the robustness of our fibrillation approach. The xylose and xylooligo yield applying these catalytic fibrils was also quantified using a temperature gradient between 33-49 °C, in 5 °C increments at pH 6. The xylose amount released using 45 °C for 24 h is elevated by 9% compared to 37 °C. However, if the fibrils are reused, 45 °C is less appropriate as the fibrils suffer a 50% efficiency decrease already after one additional repeat. The most reproducible xylose yield, while reusing the fibrils eight times, were obtained at 33 °C. At last, the fibrils were also subjected to agitation at 500 and 1,000 rpm. Surprisingly, the xylose yield was increased by 26 % after a 24 h incubation at 37 °C compared to the soluble enzymes. We concluded, that the mass transport of the heterogeneous substrate is the dominating cause for this effect.

A unified xylose release and oxidation, by a XynA/βXyl/ASD functionalized fibril cocktail was difficult to implement since the reactions have different pH and long-term temperature optima. At pH 6.0, 300-fold more ASD would be necessary to compensate the loss of activity compared to pH 9.0. However, a compromise at pH 7.5 and room temperature, which ensures the long-term integrity of fibrils equipped with ASD, reduces the rate of xylose accumulation by XynA/βXyl 11-fold. This implies that the hydrolysis of xylan would require 11 days instead of one. Nevertheless, we have tested this combination at pH 7.5 and room temperature in an open Eppendorf tube to allow continuous oxygenation of the sample, using the molar concentrations 0.4/12/120 µM of XynA/βXyl/ASD fibrils. In this reaction xylobiose and xylotriose are almost exclusively oxidized over the course of one week, whereas only minor amounts of xylose and xylonolactone were detected. Our preliminary hypothesis is that βXyl is inhibited by the fast production of xylobionolactone and xylotrionolactone. Therefore, additional modifications to the reaction conditions are necessary to shift the equilibrium towards xylonolactone.

A modular cascade setup is a more reasonable strategy that can be executed faster and requires less enzyme. The basis of this arrangement is that xylose is produced first with a XynA/βXyl cocktail at pH 6 and 37 °C. Subsequently the XynA/βXyl fibrils are removed, the pH of the substrate is adjusted to 9.0, and replaced with ASD functionalized fibrils that oxidize xylose to xylonolactone. We have also tested this strategy and found that 97% of the xylose are oxidized after 24 h at room temperature, also using an Eppendorf tube with access to air.

4.6 Producing Ready-To-Use Nanofibrils

Biotechnological applications require scales that are far greater than those produced in a research laboratory, which is a real issue, since plenty of brilliant inventions fail due to practical problems like upscaling and cost.

This is why we raised the question of choosing a suitable methodology for upscaling the production of amyloid fibrils (Paper III). Short PNF forming peptides that are chemically produced are expensive and can therefore not be produced on the scales required for industrial applications. Due to the chemicals involved for the production of synthetic peptides, the concept would also obliterate the whole idea of producing environmentally friendly materials (Diaz-Caballero et al., 2018). Another route would be to produce the proteins heterologously in *E. coli.* However, this is only an option on a laboratory scale. Since *E. coli* has a poor protein secretion machinery the cells have to be lysed, to be able to access the expressed proteins. Subsequently, purification of the amyloidogenic peptides is necessary and often requires the use of denaturants, which is both expensive and time consuming. Instead of using *E. coli* to produce foreign amyloids an elegant direction is to exploit the inherent capability if *E. coli* to form curli nanofibrils, which are essential for biofilm formation (Courchesne et al., 2017, Nguyen et al., 2014, Nussbaumer et al., 2017). The currently cheapest source for amyloidogenic proteins is mammalian, for example β-lactoglobulin from whey. Even though these proteins could be used to create hybrid materials with other nanostructures, the issue is that it is extremely inefficient and time consuming to engineer the proteins by genetic re-design. To produce other amyloids besides curli fibrils from *E. coli*, the last option is to move to other microorganisms that are known for their capability to produce high yields of proteins and which have a good protein secretion machinery. As a starting point to develop a generic recombinant host for the expression of PNF, we chose *Komagataella pastoris* (*K. pastoris*), which fulfils the above-named requirements.

In this study we inserted one copy of the gene for Sup35(1-61)-ZZ and two copies of the gene for Sup35(1-61) via homologous recombination into the genome of *K. pastoris* and obtained a new strain which we named AG2. The genes for the chimeric and carrier proteins were N-terminally linked to the α-factor, which targeted the proteins for secretion into the extracellular medium. The concept was based upon the idea that the exported proteins will aggregate into functional fibrils during the cultivation and thereby be separated from other contaminating proteins present in the medium, which will stay in solution. After successful transformation of *K. pastoris* we initially screened transformants for the production of soluble Sup35(1-61)-ZZ and Sup35(1-61), and based upon results using SDS-PAGE, concluded that the proteins were not present in soluble

fraction. Instead, we identified a pale green-yellow deposit, which appeared as an additional layer on top of the cell pellet after centrifugation of a *K. pastoris* AG2 culture. Analysis of this deposit revealed bright fluorescence with ThT, elongated fibrils using TEM, and two protein bands on an SDS-PAGE, which correlate with expected sizes for Sup35(1-61) and Sup35(1-61)-ZZ. To separate the fibrils from the *K. pastoris* cells we selectively resuspended the fibrils in saline H_2O. This is possible since the cell pellet is much heavier and denser than the fibril deposit. This approach requires minimal downstream purification and the fibrils are ready-to-use after washing with saline H_2O only. To proof the concept, we produced 35 mg per liter of cell culture of the antibody binding nanofibril.

By choosing to insert a 2:1 ratio of carrier over chimeric protein, we aimed a doping frequency of 1:0.5, which is higher than the optimal ratio 1:0.33 (Paper I). Interestingly, the material produced in the fermentor had an IgG binding capacity of 3.1 mg/mg fibril, which is 67 % more binding capacity compared the material that we have assembled using proteins expressed in *E. coli* (Paper I). In addition, the doping frequency was 1:0.12, only 1/3 of the optimized fibrils from Paper I. To account for the difference, it has to be considered that the carrier proteins were subject to C-terminal proteolytic degradation. As a result, they are 40% smaller compared to the Sup35(1-61) construct produced in *E. coli*. Additional differences are possibly explained by considering the uncertainty with respect to the concentration of Sup35(1-61) and Sup35(1-61)-ZZ. These results show that a way to obtain higher IgG binding capacities, would be to trim the peptide sequence of the carrier protein even further. Certainly, there has to be a balance between how short the carrier proteins can be and the propensity of the peptide to efficiently fibrillate in the extracellular medium. The effect of the size of the amyloidogenic peptide and the yield needs to be balanced and shortening the carrier protein should only have a minor effect on the stability of the PNF in terms of mechanical attributes and chemical resistance.

4.7 Biotechnological Context and Practical Implications

The idea that amyloid could be used as designable material was launched 18 years ago, but biotechnological implementation is still on hold. Therefore, I would like to discuss the reasons for the slow progression of the PNF technology.

With respect to amyloid, the main research is conducted on neurodegenerative diseases, which is a paramount concern for world-health. Since the same acute inducement for the discovery of practical implications of amyloid is missing, the field lags behind. Another factor that could contribute to the slow progression is that the word ‘amyloid’ is still almost exclusively

associated with disease in the public opinion. Others, who are not familiar with the field, may not be aware of the common existence of 'functional amyloid' and the advantageous properties of the material.

From a material perspective, the protein-based spider silk had a head start and was for a long time the main target of research for biotechnological utilization. Even though no negative association with respect to silk exists, research conducted for more than 40 years (Jannson, 2015) has resulted in only few prototype applications by 2018 (Salehi and Scheibel, 2018).

Compared to spider silk, amyloidogenic peptides are in many respects easier to handle and to design. The peptides grant more flexibility regarding the peptide length (2 to >100 amino acids). Furthermore, they can be specifically engineered with respect to amino acid compositions and charge distribution. If this is executed correctly, rational design of amyloidogenic peptides does not alter the fibrillation efficiency or the mechanical properties of the assembled fibrils. Finally, the peptides self-assemble into fibrils at much lower concentrations.

A biotechnological challenge that both spider-silk and amyloid materials face is that they suffer from the same reduction of mechanical stiffness when the nanofibrils are assembled into macrostructures (Kamada et al., 2017). For instance, longer amyloid fibrils are more fragile than shorter analogues (Knowles and Buehler, 2011).

On a positive note, in the past three years several extremely comprehensive reviews (see section 2.3.5) that summarize demonstrated applications of PNFs were published, which shows the accelerating interest and recognition of this material scaffold.

In the subsequent sections, I will review the functionalized nanofibrils developed in this work with respect to their biotechnological significance. At the end of section 4.7.4, I will once more highlight cost-related questions and their practical implications.

4.7.1 The Antibody Binding Nanofibril

Monoclonal antibodies (mAB) are a relatively new class of drugs, so called protein therapeutics, that are highly successful applied against inflammatory and cancer diseases (Shepard et al., 2017). The antibodies are highly specific, compared to the classical small organic compounds, and aim to activate the innate immune system. Today, more than 57 antibodies are FDA-approved, which amounts to a total market value of more than $ 100 billion per year (Grilo and Mantalaris, 2018).

Protein A Sepharose is an affinity medium distributed by GE Healthcare, and the main chromatographic method used for purification of mAB. However, the

medium is criticized for having a rather low IgG binding capacity and being expensive (Shukla et al., 2007, Kelley, 2009, Gagnon, 2012). Compared to the protein A Sepharose (drained medium) and the competing PolyBind-Z™ (PolyBatics Ltd.), the binding capacity of the ZZ-domain doped optimized Sup35(1-61) fibril is at least 20-fold higher (Paper I).

Therefore, we investigated the suitability of the fibrils for purification of human IgG from serum. In this experiment we incubated a ZZ-functionalized fibril suspension (both Sup35(1-61) and Ure2(1-80)) with the complex serum matrix. The fibrils were sedimented by centrifugation, washed thoroughly with tris-buffer (pH 8), before the IgG was eluted with a glycine-HCl buffer (pH 3). The protein contents of the different purification steps were analysed with SDS-PAGE (**Figure 14**). The purity of the eluted antibodies is almost identical to reference samples of protein A Sepharose purified human IgG. The only caveat of this protocol is leakage of small fibril fragments during elution, but which can be removed with size exclusion chromatography. Since this leakage seems to be more severe for Sup35(1-61) than for Ure2(1-80) fibrils, further improvement could be achieved by additional optimization, to create a fibril backbone that does not leak during elution.

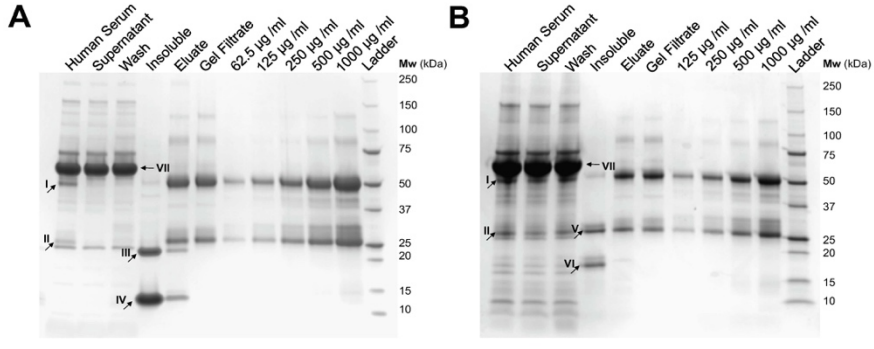

Figure 14. SDS-PAGE of the purification of human IgG from serum. The numbered arrows I-VII refer to: (I) IgG light chain, (II) IgG heavy chain, (III) Sup35(1-61)-ZZ, (IV) Sup35(1-61), (V) Ure2(1-80), (VI) Ure2(1-80)-ZZ, and (VII) Albumin. Known amounts of human IgG (Thermo Fisher) were included as a reference.

Shortly after Paper I was published, GE Healthcare introduced their next generation monoclonal antibody (mAB) purification material, MabSelect PrismA (GE Healthcare, 2018),with an binding capacity of 80 mg/mL medium. Considering that one mL of Sepharose corresponds to 250 µg of dry weight medium (Amersham Bioscience, 2003), the approximate corresponding binding capacity of MabSelect PrismA is 0.32 mg/mg (**Figure 15**). With 1.8 mg/mg, the IgG binding capacity of our material is still superior by a factor of 5.6. However, the ZZ-doped fibrils cannot compete with the optimized IgG binding domain from GE Healthcare, which has an exceptional stability. In addition, Sepharose is a well-established chromatographic medium that tolerates high flow rates and pressure. An advantage of our approach compared to the agarose beads is that the antibody binding nanofibrils do not require environmentally hazardous chemicals for cross-linking the functional domain to the matrix, as this is the case for the Sepharose affinity medium. Nevertheless, in face of this new development, it will be extremely challenging to compete with the world-wide established antibody affinity medium. Biotechnologically, our fibrils have yet another potential application. The high antibody binding capacity of our fibrils would be an excellent match to the increase the sensitivity of immunoassays (**Figure 16**) (Men et al., 2009, Men et al., 2016, Leng et al., 2010, Men et al., 2010).

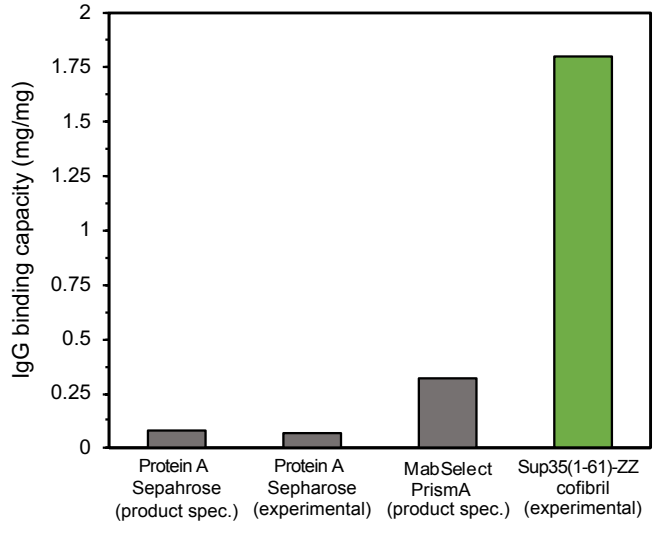

Figure 15. Experimentally determined binding capacity of protein A Sepharose (dry weight) and Sup35-ZZ fibrils (doping frequency 1:0.33).

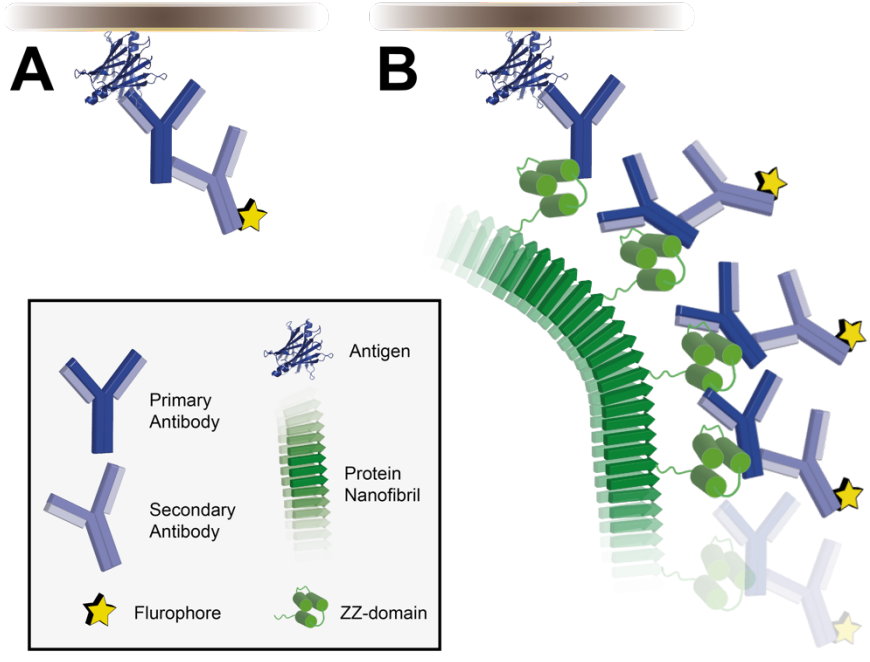

Figure 16. (A) Indirect Immunoassay: An antigen is adsorbed onto an immunoplate and recruits the primary antibody. The primary antibody is recognized by the secondary antibody, which is conjugated with a fluorophore, thus generating a signal. (B) Using the ZZ-doped PNFs can enhance the signal, and thus the sensitivity by linking many more signal generating secondary antibodies to one antigen.

4.7.2 Hydrolysis of Antibiotic Contaminations

The release of non-metabolized antibiotics into the wastewater and ultimately into lakes and oceans is a major environmental hazard (Baran et al., 2018). Furthermore, this practice favours the development of multi-resistant bacteria, which is a world-wide concern for public health (Zhang et al., 2016). Current methods to degrade pharmaceutical contaminations include sludge bioreactors, UV/H_2O_2 wastewater treatment, and coagulation (Baran et al., 2018, Guo et al., 2018, Zhang et al., 2016). The efficiencies of pharmaceutical removal are often suboptimal (20-70%) and they produce several non-characterized by-products. Certainly, the wastewater reprocessing is an extremely price sensitive market, which requires new affordable, well-characterized, and environmentally friendly solutions.

The TEM1 functionalized fibrils degrade β-lactam antibiotics such as penicillin and ampicillin (Paper II). These and other enzymes that can specifically degrade pharmaceuticals could be used in synergy for an environmentally friendly method for wastewater treatment. The advantage using an enzyme cocktail compared to chemical methods is that the biocatalysts yield known products and by-products. However, a practical application of the enzyme functionalized fibrils for wastewater treatment would require enormous quantities of the material. To implement these and similar applications a major research aim should be to develop the methodology for producing functionalized amyloid fibrils for a reasonable price (Paper III).

The enzymatic nanofibrils could be utilized to construct pharmaceutical degrading membranes, but the risk for immediate clogging is extremely high, if the water is not thoroughly pre-filtered. An alternative would be to fill a pool with a fibril suspension, that is allowed to sediment, when the reaction is done. In any case, since it is to date not possible to produce the quantities required, this method should be reconsidered in the future.

4.7.3 Enzyme Immobilization and Processing of Xylan Biomass

A reoccurring argument for reusing enzymes is that the cost of the catalysed bioprocess could be significantly reduced (Es et al., 2015). To render enzymes reusable, they have to be coupled onto a solid support to attain an irreversible separation of the biocatalyst and the substrate solution. Other typical mentioned motivations that intend to promote enzyme immobilization in industrial settings is the simplicity of post-catalytic enzyme removal and a higher enzyme tolerance against harsh conditions. Therefore, the technique of immobilizing enzymes on solid materials is a widely researched subject within biotechnology that has produced hundreds of applications in recent years (Zhou and Hartmann, 2013). This research has also generated a large array of different immobilization strategies and promoted the development of materials that are appropriate for enzyme coupling (Datta et al., 2013). In particular, nanoscale supports have an advantage over classical porous materials as they ensure a high functional density (Min and Yoo, 2014). Even though this positively enforced arguments are repeatedly used, only very few applications of immobilized enzymes have been commercialized (DiCosimo et al., 2013). The authors argue that the main justification to utilize immobilized enzymes – a cost reduction – is in the majority of cases not relevant, because industrial enzymes are not expensive and cost only between 50-500 $/kg (see also section 4.7.4). Instead, the process of enzyme immobilization is the cause for a substantial cost, which includes the cost of the immobilization matrix, the cross-linking chemicals, the time needed

for the immobilization process, and costs related to alterations of enzyme kinetic properties.

Our recent success to produce ready-to-use functionalized nanofibrils with *K. pastoris* while cultivating our yeast-strain in a fermentor (Paper III), could be an important discovery that has the potential to simultaneously accomplish enzyme production and immobilization. Hence, the additional time and cost for immobilizing enzymes would be omitted, which could make the reusable biocatalysts relevant for an increasing number of biotechnological applications. Furthermore, the demand to develop environmentally-friendly functional materials would also be fulfilled. In light of this progress, we wanted to study the potential of amyloid fibrils as a tool to assemble complete catalytic cascade of immobilized enzymes that synthetize important chemicals.

Alternatives to chemical methods usually rely on the utilization of engineered microorganisms, but the development of these cellular factories demand hundreds of accumulated working years (Hodgman and Jewett, 2012, Korman et al., 2017). On the contrary, the development of cell-free biocatalytic cascades is expected to be much faster. Other advantages of cell-free catalytic systems become evident in Paper IV. In this study it was simple to identify problematic steps in the catalytic cascade, adjust the relative enzyme concentrations to maximize the product yield, optimize the reaction conditions, and develop rational strategies that accelerate the process of biocatalysis.

The catalytic cascade in Paper IV involved the enzymes XynA, βXyl and ASD, which we specifically chose, to explore the option of designing biomass processing PNF. Mainly, the reason to utilize biomass is to reduce our societies dependency upon petrol-based chemicals (McKenna et al., 2015). Thus, the consumption of xylan for this purpose, the second most abundant carbohydrate polymer after cellulose, celebrates a growing interest (Michelin et al., 2012). It is therefore no surprise that the synergetic catalytic action of xylanase and β-xylosidase is the target of several recent studies (Biely et al., 2016, Yang et al., 2014, Malgas et al., 2017). The catalytic hydrolysis of xylan is also important to enable fast enzymatic degradation of cellulose, since hemicellulose inhibits cellulases (Qing and Wyman, 2011). In conclusion, a combined cocktail of PNFs functionalized with cellulases, xylanases, glycosidases and xylosidases could become handy to process biomass for the production of second-generation biofuels. Since biofuel production is a very price sensitive market (Losordo et al., 2016) the process could profit from cheap ready-to-use immobilized and reusable enzymes.

4.7.4 Cost Perspective

The following discussion on the cost for producing the PNFs will be limited to the antibody binding fibrils (Paper I & III). The motivation is that there are clear cost-aims set by the competitor GE Healthcare. Furthermore, the results described in Paper III were obtained with the antibody binding PNFs, which allow us to make a rough cost estimation. Finally, the discussion of this particular material is highly relevant to us, since we recently submitted a patent application to protect our invention (Härd et al., 2016).

The cheapest proteins available today are soy bean protein and cellulases, which can be produced in the range of 1-25 $/kg (Liu et al., 2016). However, this price is only valid for rough enzyme broths. Certainly, if protein purification is required for the intended application, the cost is increased substantially. Industrial and medical proteins are produced in various recombinant hosts using *E. coli*, *K. pastoris*, *Aspergillus niger*, *Bacillus subtilis*, *Trichoderma reesi*, and mammalian cell lines. The production levels for these proteins are in the range of 4 mg/l of cell culture (Protein-glutamine γ-glutamyltransferase), 4 g/l (Insulin), 22 g/l (β-Galactosidase), to 100 g/l (Cellulase) (Spohner et al., 2015, Shin et al., 1997, Seiboth et al., 2011). A 25,000-fold difference between the production yields of this narrow selection of industrial proteins, shows that the inquiry of a minimum production yield for PNF to offer a competitive product in terms of cost, is very much dependent upon the application.

The antibody binding material is intended to be applied as a matrix for mAB purification and to improve the sensitivity of immunodetection assays. GE Healthcare will sell their new affinity medium MabSelect PrismA, for the purification of mAB, for not less than $ 28 per ml[4]. When Sepharose is dried, the weight of the material is reduced by a factor of 4. Accordingly, the selling price can be estimated to 112 $/g. However, this allows no conclusion with respect to the cost of production for the affinity medium since this is a highly sensitive information and not publicly available.

Considering that the production yield of the antibody binding nanofibrils is 35 mg/l and one batch in a 5L fermentor costs approximately $ 714 (**Table 4 and 5)**, to produce one gram would currently cost $ 4,080, which is obviously not reasonable for an antibody purification material. However, to improve an immunodetection assay kit (for example TNFα, 96 well plate for $ 460)[5], will not consume more than 5 µg fibrils per well (Men et al., 2009). Thus, the

4. Based on an estimate from the precursor material MabSelect SuRe (GE Healthcare) sold by Merck. (https://www.sigmaaldrich.com/catalog/product/sigma/ge17543801?lang=en&region=SE, last accessed August 9th, 2018)

5. Assay from Thermo Fisher Scientific (https://www.thermofisher.com/elisa/product/TNF-alpha-Human-ELISA-Kit/KHC3011, last accessed August 9th, 2018)

Table 4. Estimation of the cost to run a 5L fermentor on a laboratory scale.

	cost ($)/ batch	Time (h)
Fermentor (5L)	600	48
Laboratory Staff	100	4
Cultivation Medium	14	/
Sum	714	

The prices are rough estimates based upon the equipment and the facilities in the laboratory from Mats Sandgren.

Table 5. Cost of YPD-Medium components per liter of liquid culture medium.

Component	$ / kg dry weight	g / l	$ / l
Peptone	92	20	1.84
Yeast extract	48	10	0.68
Glucose	14	20	0.28
Sum			2.8

The calculation is based upon medium components from Formedium. A cost of 2.8 $/l of medium corresponds to $ 14 for a 5L fermenter.

additional cost for the fibrils of a 96 well plate kit is $ 1.95, and probably competitive with respect to estimated 100-fold improvement of the sensitivity.

To make the PNF technology also commercially feasible for applications that require several g or kg of the material, the production has to be scaled to industrial size fermenters. Unquestionably, the price per liter of culture in an industrial scale fermentor is reduced substantially, but I cannot refer to a published estimate from biotechnological companies, since the cost is confidential. However, the cost can be roughly estimated by considering that a biofuel plant by DuPont can produce second generation bioethanol currently at $ 2.9 per liter ethanol (Losordo et al., 2016). The basis of second-generation bioethanol production is the release of glucose from cellulose by enzymatic hydrolysis. A reasonable assumption is that a 3% (w/w, 30 g) enzyme dosage is used to hydrolyze cellulose (Novozymes, 2010). Furthermore, in the best-case scenario 0.5-liter ethanol can be obtained from one kg cellulose (Aditiya et al., 2016). Thus, 60 g enzyme are consumed to obtain one liter of ethanol. With the knowledge that enzymes account for at least 40 % of the cost of bioethanol production (Tiwari et al., 2018), we can conclude that 60 g cellulase cost $ 1.2.

Assuming that *Trichoderma reesi* expresses 100 g cellulase per liter of cell culture means that cultivation of one liter in an industrial size fermentor should not cost more than $ 0.7.

A reasonable aim is to obtain production of the functionalized materials in a cost competitive range above 1 g/l. These expression levels in combination with the estimated cost of a cultivation in an industrial size fermentor, would all of a sudden make applications for antibody purification or similar feasible.

To engineer *K. pastoris AG2* further, time needs to be spent on integrating enough copies into the high expression positions of the genome, and to optimize the cultivation conditions. Additional strategies to engineer the PNF producer is to remove antibiotic resistant makers, proteases, and genes for non-essential proteins in order to save energy for the target protein. This task can be done with the newly developed and well documented CRIPSR/Cas9 genome editing technology.

If these attempts fail, it will be inevitable to screen additional production hosts. The minimal requirements are that the cultivation is scalable, and that simple media components are needed for efficient growth of the microorganisms. These requirements exclude cell-free systems as well as mammalian and insect cell expression systems. As an alternative to *E. coli*, *Bacillus subtilis* could be a feasible option since the bacteria grow rapidly and can produce extracellular protein above the g/L range (Zhang et al., 2017, Westers et al., 2004). Other more exotic options are *Lactococcus lactis* (Jorgensen et al., 2014), or *Ralstonia eutropha* that can also express up to 10 g/L of heterologous extracellular protein (Barnard et al., 2004). A greater effort would be to engineer filamentous fungi. *Aspergillus niger* and *Trichoderma reesi* are the workhorses for industrial cellulase and can produce amounts exceeding 100 g/L. However, it is to date not possible to reach these expression levels for non-cellulase heterologous proteins (Nevalainen and Peterson, 2014, Su et al., 2012). A better choice would be to employ *Myceliophthora thermophila* since this fungi can effectively produce heterologous protein in the g/L range (Hans et al., 2011).

To find a suitable expression host and engineer the microorganism in a way to get more than 1 g/L is a time and money-consuming task, that is mostly of industrial relevance and must be executed together with industrial partners.

5 Concluding Remarks and Future Perspectives

I hope that I could convince the reader of this work, that the development of PNF technology is a worthy research investment that could provide novel solutions to current biotechnological aims of modern society. Among others, the major aims of biotechnological applications can be grouped into five categories: 1) the development of sustainable synthesis pathways, using biocatalysts or microorganisms, for the production of fine chemicals in order to reduce the environmental impact of industry; 2) to assemble biocompatible and degradable materials that can reduce society's dependency on synthetic plastics; 3) to produce designable self-assembling materials by applying the bottom-up approach of nanotechnology; 4) to improve healthcare and diagnostics; and 5) to minimize the anthropogenic environmental impact in general. So far, PNF materials developed on laboratory scale promote all of the above-mentioned aims. Functionalized fibrils can capture CO_2 ($\rightarrow$ 5), are used to enrich rare earth metals ($\rightarrow$ 3, 5), are applied to assemble conducting nanowires ($\rightarrow$ 3), and are novel alternatives to synthetic plastics ($\rightarrow$ 2) (Ye et al., 2018). Furthermore, in this work I have developed fibrils that can be employed as an antibody purification matrix ($\rightarrow$ 4), serve as a filter for antibiotic degradation ($\rightarrow$ 5), and process xylan biomass using an immobilized enzymatic cascade ($\rightarrow$ 1). Nevertheless, the PNF technology is in some aspects still in its infancy, and requires additional developmental work to make the technology commercially competitive.

An imminent study should evaluate how the degree of functionality influences the mechanical properties of amyloid fibrils. In the next stage a thorough investigation may focus on the difficulty to transfer the advantageous material properties of PNF to structures with macro-morphologies. In the best-case scenario, macro-structures should possess the same mechanical stiffness as the individual nanofibril. Furthermore, a targeted study to elucidate and confirm

the safety of functional amyloid, especially for *in vivo* applications, is inevitable. Finally, the production levels of functionalized ready-to-use PNF for different applications in order to be profitable should be meticulously evaluated. The final task of upscaling the production of the PNF is a major effort that needs to be tackled together with industrial partners.

In summary, amyloid fibrils are a versatile material. The difficulty is not to design new materials, but to make the transition from lab-scale proof of concept deigns to commercially competitive solutions for current biotechnological problems. To accelerate this transition, close collaboration with industry is necessary, to develop the technology for specific relevant purposes.

References

ABELEIN, A., JARVET, J., BARTH, A., GRASLUND, A. & DANIELSSON, J. 2016. Ionic Strength Modulation of the Free Energy Landscape of A beta(40) Peptide Fibril Formation. *Journal of the American Chemical Society,* 138**,** 6893-6902.

ADAMCIK, J. & MEZZENGA, R. 2018. Amyloid Polymorphism in the Protein Folding and Aggregation Energy Landscape. *Angewandte Chemie-International Edition,* 57**,** 8370-8382.

ADITIYA, H. B., MAHLIA, T. M. I., CHONG, W. T., NUR, H. & SEBAYANG, A. H. 2016. Second generation bioethanol production: A critical review. *Renewable & Sustainable Energy Reviews,* 66**,** 631-653.

AGNARSSON, I., KUNTNER, M. & BLACKLEDGE, T. A. 2010. Bioprospecting Finds the Toughest Biological Material: Extraordinary Silk from a Giant Riverine Orb Spider. *Plos One,* 5.

AMERICAN CHEMICAL SOCIETY. 2018. *American Chemical Society National Historic Chemical Landmarks. Bakelite: The World's First Synthetic Plastic* [Online]. Available: http://www.acs.org/content/acs/en/education/whatischemistry/landmarks/bakelite.html [Accessed 2018-07-20].

AMERSHAM BIOSCIENCE. 2003. *Blue Sepharose CL-6B* [Online]. Available: https://www.gelifesciences.co.jp/tech_support/manual/pdf/71708200ae.pdf [Accessed 24th August 2018].

ANDERSSON, M., JIA, Q. P., ABELLA, A., LEE, X. Y., LANDREH, M., PURHONEN, P., HEBERT, H., TENJE, M., ROBINSON, C. V., MENG, Q., PLAZA, G. R., JOHANSSON, J. & RISING, A. 2017. Biomimetic spinning of artificial spider silk from a chimeric minispidroin. *Nature Chemical Biology,* 13**,** 262-264.

AROSIO, P., KNOWLES, T. P. J. & LINSE, S. 2015. On the lag phase in amyloid fibril formation. *Physical Chemistry Chemical Physics,* 17**,** 7606-7618.

BADER, R., BAMFORD, R., ZURDO, J., LUISI, B. F. & DOBSON, C. M. 2006. Probing the mechanism of amyloidogenesis through a tandem repeat of the PI3-SH3 domain suggests a generic model for protein aggregation and fibril formation. *Journal of Molecular Biology,* 356**,** 189-208.

BALAJI, A. B., PAKALAPATI, H., KHALID, M., WALVEKAR, R. & SIDDIQUI, H. 2018. Natural and synthetic biocompatible and biodegradable polymers. *In:* SHIMPI, N. G. (ed.) *Biodegradable and Biocompatible Polymer Composites.* Woodhead Publishing.

BALCHIN, D., HAYER-HARTL, M. & HARTL, F. U. 2016. In vivo aspects of protein folding and quality control. *Science,* 353.

BALDWIN, A. J., BADER, R., CHRISTODOULOU, J., MACPHEE, C. E., DOBSON, C. M. & BARKER, P. D. 2006. Cytochrome display on amyloid fibrils. *J Am Chem Soc,* 128**,** 2162-2163.

BARAN, W., ADAMEK, E., JAJKO, M. & SOBCZAK, A. 2018. Removal of veterinary antibiotics from wastewater by electrocoagulation. *Chemosphere,* 194**,** 381-389.

BARNARD, G. C., HENDERSON, G. E., SRINIVASAN, S. & GERNGROSS, T. U. 2004. High level recombinant protein expression in Ralstonia eutropha using T7 RNA polymerase based amplification. *Protein Expression and Purification,* 38**,** 264-271.

BAUER, F., BERTINETTI, L., MASIC, A. & SCHEIBEL, T. 2012. Dependence of Mechanical Properties of Lacewing Egg Stalks on Relative Humidity. *Biomacromolecules,* 13**,** 3730-3735.
BAXA, U., KELLER, P. W., CHENG, N. Q., WALL, J. S. & STEVEN, A. C. 2011. In Sup35p filaments (the [PSI plus] prion), the globular C-terminal domains are widely offset from the amyloid fibril backbone. *Molecular Microbiology,* 79**,** 523-532.
BAXA, U., ROSS, P. D., WICKNER, R. B. & STEVEN, A. C. 2004. The N-terminal prion domain of Ure2p converts from an unfolded to a thermally resistant conformation upon filament formation. *Journal of Molecular Biology,* 339**,** 259-264.
BAXA, U., SPERANSKY, V., STEVEN, A. C. & WICKNER, R. B. 2002. Mechanism of inactivation on prion conversion of the Saccharomyces cerevisiae Ure2 protein. *Proceedings of the National Academy of Sciences of the United States of America,* 99**,** 5253-5260.
BAXA, U., TAYLOR, K. L., WALL, J. S., SIMON, M. N., CHENG, N. Q., WICKNER, R. B. & STEVEN, A. C. 2003. Architecture of Ure2p prion filaments - The N-terminal domains form a central core fiber. *Journal of Biological Chemistry,* 278**,** 43717-43727.
BIELY, P., SINGH, S. & PUCHART, V. 2016. Towards enzymatic breakdown of complex plant xylan structures: State of the art. *Biotechnology Advances,* 34**,** 1260-1274.
BITTENCOURT, D. M. D. 2016. Spider Silks and Their Biotechnological Applications. *Short Views on Insect Genomics and Proteomics, Vol 2: Insect Proteomics,* 4**,** 211-227.
BOLISETTY, S. & MEZZENGA, R. 2016. Amyloid-carbon hybrid membranes for universal water purification. *Nat Nanotechnol,* 11**,** 365-71.
BONSER, R. H. C. 2000. The Young's modulus of ostrich claw keratin. *Journal of Materials Science Letters,* 19**,** 1039-1040.
BOURGOIS, T. M., NGUYEN, D. V., SANSEN, S., ROMBOUTS, S., BELIEN, T., FIERENS, K., RAEDSCHELDERS, G., RABIJNS, A., COURTIN, C. M., DELCOUR, J. A., VAN CAMPENHOUT, S. & VOLCKAERT, G. 2007. Targeted molecular engineering of a family 11 endoxylanase to decrease its sensitivity towards Triticum aestivum endoxylanase inhibitor types. *J Biotechnol,* 130**,** 95-105.
BUEHLER, M. J. & YUNG, Y. C. 2010. How protein materials balance strength, robustness, and adaptability. *Hfsp Journal,* 4**,** 26-40.
CEN, L., LIU, W., CUI, L., ZHANG, W. J. & CAO, Y. L. 2008. Collagen tissue engineering: Development of novel biomaterials and applications. *Pediatric Research,* 63**,** 492-496.
CHANNON, K. J., DEVLIN, G. L., MAGENNIS, S. W., FINLAYSON, C. E., TICKLER, A. K., SILVA, C. & MACPHEE, C. E. 2008. Modification of fluorophore photophysics through peptide-driven self-assembly. *Journal of the American Chemical Society,* 130**,** 5487-5491.
CHATANI, E., LEE, Y. H., YAGI, H., YOSHIMURA, Y., NAIKI, H. & GOTO, Y. 2009. Ultrasonication-dependent production and breakdown lead to minimum-sized amyloid fibrils. *Proceedings of the National Academy of Sciences of the United States of America,* 106**,** 11119-11124.
CHEN, B., RETZLAFF, M., ROOS, T. & FRYDMAN, J. 2011. Cellular Strategies of Protein Quality Control. *Cold Spring Harbor Perspectives in Biology,* 3**,** 1-14.
CHEN, Z., GANDHI, U., LEE, J. & WAGONER, R. H. 2016. Variation and consistency of Young's modulus in steel. *Journal of Materials Processing Technology,* 227**,** 227-243.
CHERNY, I. & GAZIT, E. 2008. Amyloids: Not Only Pathological Agents but Also Ordered Nanomaterials. *Angewandte Chemie International Edition,* 47**,** 4062-4069.
CHERNY, I., ROCKAH, L., LEVY-NISSENBAU, O., GOPHNA, U., RON, E. Z. & GAZIT, E. 2005. The formation of Escherichia coli curli amyloid fibrils is mediated by prion-like peptide repeats. *Journal of Molecular Biology,* 352**,** 245-252.
CHITI, F. & DOBSON, C. M. 2006. Protein misfolding, functional amyloid, and human disease. *Annual Review of Biochemistry,* 75**,** 333-366.
COHEN, S. I. A., LINSE, S., LUHESHI, L. M., HELLSTRAND, E., WHITE, D. A., RAJAH, L., OTZEN, D. E., VENDRUSCOLO, M., DOBSON, C. M. & KNOWLES, T. P. J. 2013. Proliferation of amyloid-beta 42 aggregates occurs through a secondary nucleation mechanism. *Proceedings of the National Academy of Sciences of the United States of America,* 110**,** 9758-9763.
COLLINS, S. R., DOUGLASS, A., VALE, R. D. & WEISSMAN, J. S. 2004. Mechanism of prion propagation: Amyloid growth occurs by monomer addition. *PLOS Biology,* 2**,** 1582-1590.
COLVIN, M. T., SILVERS, R., NI, Q. Z., CAN, T. V., SERGEYEV, I., ROSAY, M., DONOVAN, K. J., MICHAEL, B., WALL, J., LINSE, S. & GRIFFIN, R. G. 2016. Atomic Resolution

Structure of Monomorphic Abeta42 Amyloid Fibrils. *Journal of the American Chemical Society,* 138**,** 9663-9674.
CORREA, J. M., GRACIANO, L., ABRAHAO, J., LOTH, E. A., GANDRA, R. F., KADOWAKI, M. K., HENN, C. & SIMAO, R. D. G. 2012. Expression and Characterization of a GH39 beta-Xylosidase II from Caulobacter crescentus. *Applied Biochemistry and Biotechnology,* 168**,** 2218-2229.
COURCHESNE, N. M. D., DURAJ-THATTE, A., TAY, P. K. R., NGUYEN, P. Q. & JOSHI, N. S. 2017. Scalable Production of Genetically Engineered Nanofibrous Macroscopic Materials via Filtration. *Acs Biomaterials Science & Engineering,* 3**,** 733-741.
DATTA, S., CHRISTENA, L. R. & RAJARAM, Y. R. S. 2013. Enzyme immobilization: an overview on techniques and support materials. *3 Biotech,* 3**,** 1-9.
DEPACE, A. H., SANTOSO, A., HILLNER, P. & WEISSMAN, J. S. 1998. A critical role for amino-terminal glutamine/asparagine repeats in the formation and propagation of a yeast prion. *Cell,* 93**,** 1241-1252.
DÍAZ-CABALLERO, M., FERNANDEZ, M. R., NAVARRO, S. & VENTURA, S. 2018. Prion-Based Nanomaterials and their Emerging Applications. *Prion***,** 1-8.
DIAZ-CABALLERO, M., NAVARRO, S., FUENTES, I., TEIXIDOR, F. & VENTURA, S. 2018. Minimalist Prion-Inspired Polar Self-Assembling Peptides. *ACS Nano,* 12**,** 5394-5407.
DICOSIMO, R., MCAULIFFE, J., POULOSE, A. J. & BOHLMANN, G. 2013. Industrial use of immobilized enzymes. *Chemical Society Reviews,* 42**,** 6437-6474.
ELFWING, A., BACKLUND, F. G., MUSUMECI, C., INGANAS, O. & SOLIN, N. 2015. Protein nanowires with conductive properties. *Journal of Materials Chemistry C,* 3**,** 6499-6504.
ES, I., VIEIRA, J. D. G. & AMARAL, A. C. 2015. Principles, techniques, and applications of biocatalyst immobilization for industrial application. *Applied Microbiology and Biotechnology,* 99**,** 2065-2082.
FOWLER, D. M., KOULOV, A. V., BALCH, W. E. & KELLY, J. W. 2007. Functional amyloid - from bacteria to humans. *Trends in Biochemical Sciences,* 32**,** 217-224.
GAGNON, P. 2012. Technology trends in antibody purification. *Journal of Chromatography A,* 1221**,** 57-70.
GE HEALTHCARE. 2018. *MabSelect PrismA* [Online]. Available: https://www.gelifesciences.co.jp/products/bioprocess/pdf/KA553200917DF_PrismA_datafile.pdf [Accessed 24th July 2018].
GEYER, R., JAMBECK, J. R. & LAW, K. L. 2017. Production, use, and fate of all plastics ever made. *Science Advances,* 3**,** e1700782.
GILBERT, M. 2017. Plastics Materials: Introduction and Historical Development. *In:* GILBERT, M. (ed.) *Brydson's Plastics Materials*. Butterworth-Heinemann.
GIRI, K., BHATTACHARYYA, N. P. & BASAK, S. 2007. pH-dependent self-assembly of polyalanine peptides. *Biophysical Journal,* 92**,** 293-302.
GLOVER, J. R., KOWAL, A. S., SCHIRMER, E. C., PATINO, M. M., LIU, J. J. & LINDQUIST, S. 1997. Self-seeded fibers formed by Sup35, the protein determinant of [PSI+], a heritable prion-like factor of S-cerevisiae. *Cell,* 89**,** 811-819.
GORKOVSKIY, A., THURBER, K. R., TYCKO, R. & WICKNER, R. B. 2014. Locating folds of the in-register parallel beta-sheet of the Sup35p prion domain infectious amyloid. *Proceedings of the National Academy of Sciences of the United States of America,* 111**,** e4615-e4622.
GREEN, D. K. J. W. D. 1999. *Mechanical properties of wood, Chapter 4. Wood handbook : wood as an engineering material, FPL-GTR-113*, Madison, WI : USDA Forest Service, Forest Products Laboratory.
GRILO, A. L. & MANTALARIS, A. 2018. The Increasingly Human and Profitable Monoclonal Antibody Market. *Trends in Biotechnology*.
GUO, J. X., FARID, M. U., LEE, E. J., YAN, D. Y. S., JEONG, S. & AN, A. K. 2018. Fouling behavior of negatively charged PVDF membrane in membrane distillation for removal of antibiotics from wastewater. *Journal of Membrane Science,* 551**,** 12-19.
HANS, V., VIVI, J., J., P. P., V., G. A., T., O. P., ROB, J., JEFFREY, B., JAAP, V., P., S. A., A., E. M., C., V. J. & JAN, W. 2011. RESEARCH: Development of a mature fungal technology and production platform for industrial enzymes based on a Myceliophthora thermophila isolate, previously known as Chrysosporium lucknowense C1. *Industrial Biotechnology,* 7**,** 214-223.
HÄRD, T., SCHMUCK, B. & SANDGREN, M. 2016. *Antibody binding nanofibrils*. WO/2017/200461.

HAUSER, C. A., MAURER-STROH, S. & MARTINS, I. C. 2014. Amyloid-based nanosensors and nanodevices. *Chemical Society Reviews,* 43**,** 5326-5345.
HELLSTRAND, E., BOLAND, B., WALSH, D. M. & LINSE, S. 2010. Amyloid beta-Protein Aggregation Produces Highly Reproducible Kinetic Data and Occurs by a Two-Phase Process. *ACS Chemical Neuroscience,* 1**,** 13-18.
HODGMAN, C. E. & JEWETT, M. C. 2012. Cell-free synthetic biology: thinking outside the cell. *Metabolic Engineering,* 14**,** 261-9.
HOLMES, T. C., DE LACALLE, S., SU, X., LIU, G. S., RICH, A. & ZHANG, S. G. 2000. Extensive neurite outgrowth and active synapse formation on self-assembling peptide scaffolds. *Proceedings of the National Academy of Sciences of the United States of America,* 97**,** 6728-6733.
HUDALLA, G. A., SUN, T., GASIOROWSKI, J. Z., HAN, H. F., TIAN, Y. F., CHONG, A. S. & COLLIER, J. H. 2014. Gradated assembly of multiple proteins into supramolecular nanomaterials. *Nature Materials,* 13**,** 829-836.
JANNSON, R. 2015. *Strategies for functionalization of recombinant spider silk.*
JANSSON, R., COURTIN, C. M., SANDGREN, M. & HEDHAMMAR, M. 2015. Rational Design of Spider Silk Materials Genetically Fused with an Enzyme. *Advanced Functional Materials,* 25**,** 5343-5352.
JANSSON, R., THATIKONDA, N., LINDBERG, D., RISING, A., JOHANSSON, J., NYGREN, P. A. & HEDHAMMAR, M. 2014. Recombinant Spider Silk Genetically Functionalized with Affinity Domains. *Biomacromolecules,* 15**,** 1696-1706.
JEBALI, A., NAYERI, E. K., ROOHANA, S., AGHAEI, S., GHAFFARI, M., DALIRI, K. & FUENTE, G. 2017. Nano-carbohydrates: Synthesis and application in genetics, biotechnology, and medicine. *Advances in Colloid and Interface Science,* 240**,** 1-14.
JORGENSEN, C. M., VRANG, A. & MADSEN, S. M. 2014. Recombinant protein expression in Lactococcus lactis using the P170 expression system. *Fems Microbiology Letters,* 351**,** 170-178.
KAMADA, A., MITTAL, N., SODERBERG, L. D., INGVERUD, T., OHM, W., ROTH, S. V., LUNDELL, F. & LENDEL, C. 2017. Flow-assisted assembly of nanostructured protein microfibers. *Proceedings of the National Academy of Sciences of the United States of America,* 114**,** 1232-1237.
KELLEY, B. 2009. Industrialization of mAb production technology The bioprocessing industry at a crossroads. *Mabs,* 1**,** 443-452.
KHAN, M. S., BHAT, S. A., TABREZ, S., ALAMA, M. N., ALSENAIDY, M. A. & AL-SENAIDY, A. M. 2016. Denaturation induced aggregation in alpha-crystallin: differential action of chaotropes. *Journal of Molecular Recognition,* 29**,** 536-543.
KING, C. Y. 2001. Supporting the structural basis of prion strains: induction and identification of [PSI] variants. *Journal of Molecular Biology,* 307**,** 1247-60.
KING, C. Y. & DIAZ-AVALOS, R. 2004. Protein-only transmission of three yeast prion strains. *Nature,* 428**,** 319-323.
KLEMENT, K., WIELIGMANN, K., MEINHARDT, J., HORTSCHANSKY, P., RICHTER, W. & FANDRICH, M. 2007. Effect of different salt ions on the propensity of aggregation and on the structure of Alzheimer's A beta(1-40) amyloid fibrils. *Journal of Molecular Biology,* 373**,** 1321-1333.
KNOBLAUCH, M. & PETERS, W. S. 2004. Biomimetic actuators: where technology and cell biology merge. *Cellular and Molecular Life Sciences,* 61**,** 2497-2509.
KNOWLES, T. P., FITZPATRICK, A. W., MEEHAN, S., MOTT, H. R., VENDRUSCOLO, M., DOBSON, C. M. & WELLAND, M. E. 2007. Role of intermolecular forces in defining material properties of protein nanofibrils. *Science,* 318**,** 1900-1903.
KNOWLES, T. P. J. & BUEHLER, M. J. 2011. Nanomechanics of functional and pathological amyloid materials. *Nature Nanotechnology,* 6**,** 469-479.
KNOWLES, T. P. J. & MEZZENGA, R. 2016. Amyloid Fibrils as Building Blocks for Natural and Artificial Functional Materials. *Advanced Materials,* 28**,** 6546-6561.
KNOWLES, T. P. J., OPPENHEIM, T. W., BUELL, A. K., CHIRGADZE, D. Y. & WELLAND, M. E. 2010. Nanostructured films from hierarchical self-assembly of amyloidogenic proteins. *Nature Nanotechnology,* 5**,** 204-207.
KOBAYASHI, N., YANASE, K., SATO, T., UNZAI, S., HECHT, M. H. & ARAI, R. 2016. Self-Assembling Nano-Architectures Created from a Protein Nano-Building Block Using an Intermolecularly Folded Dimeric de Novo Protein. *Protein Science,* 25**,** 48-49.

KODAMA, H., MATSUMURA, S., YAMASHITA, T. & MIHARA, H. 2004. Construction of a protein array on amyloid-like fibrils using co-assembly of designed peptides. *Chemical Communications*, 2876-2877.

KORMAN, T. P., OPGENORTH, P. H. & BOWIE, J. U. 2017. A synthetic biochemistry platform for cell free production of monoterpenes from glucose. *Nature Communications,* 8, 15526.

KOUTSOPOULOS, S., UNSWORTH, L. D., NAGAI, Y. & ZHANG, S. G. 2009. Controlled release of functional proteins through designer self-assembling peptide nanofiber hydrogel scaffold. *Proceedings of the National Academy of Sciences of the United States of America,* 106, 4623-4628.

LENG, Y., WEI, H. P., ZHANG, Z. P., ZHOU, Y. F., DENG, J. Y., CUI, Z. Q., MEN, D., YOU, X. Y., YU, Z. N., LUO, M. & ZHANG, X. E. 2010. Integration of a Fluorescent Molecular Biosensor into Self-Assembled Protein Nanowires: A Large Sensitivity Enhancement. *Angewandte Chemie-International Edition,* 49, 7243-7246.

LI, C. X. & MEZZENGA, R. 2012. Functionalization of Multiwalled Carbon Nanotubes and Their pH-Responsive Hydrogels with Amyloid Fibrils. *Langmuir,* 28, 10142-10146.

LI, D., JONES, E. M., SAWAYA, M. R., FURUKAWA, H., LUO, F., IVANOVA, M., SIEVERS, S. A., WANG, W. Y., YAGHI, O. M., LIU, C. & EISENBERG, D. S. 2014. Structure-Based Design of Functional Amyloid Materials. *Journal of the American Chemical Society,* 136, 18044-18051.

LI, Z. H., WANG, J., LI, Y. X., LIU, X. W. & YUAN, Q. 2018. Self-assembled DNA nanomaterials with highly programmed structures and functions. *Materials Chemistry Frontiers,* 2, 423-436.

LILLY, M. D., HORNBY, W. E. & CROOK, E. M. 1966. The kinetics of carboxymethylcellulose--ficin in packed beds. *The Biochemical Journal,* 100, 718-23.

LIU, G., ZHANG, J. & BAO, J. 2016. Cost evaluation of cellulase enzyme for industrial-scale cellulosic ethanol production based on rigorous Aspen Plus modeling. *Bioprocess and Biosystems Engineering,* 39, 133-140.

LOSORDO, Z., MCBRIDE, J., VAN ROOYEN, J., WENGER, K., WILLIES, D., FROEHLICH, A., MACEDO, I. & LYND, L. 2016. Cost competitive second-generation ethanol production from hemicellulose in a Brazilian sugarcane biorefinery. *Biofuels Bioproducts & Biorefining-Biofpr,* 10, 589-602.

LOVEDAY, S. M., SU, J. H., RAO, M. A., ANEMA, S. G. & SINGH, H. 2011. Effect of Calcium on the Morphology and Functionality of Whey Protein Nanofibrils. *Biomacromolecules,* 12, 3780-3788.

LUHRS, T., RITTER, C., ADRIAN, M., RIEK-LOHER, D., BOHRMANN, B., DOELI, H., SCHUBERT, D. & RIEK, R. 2005. 3D structure of Alzheimer's amyloid-beta(1-42) fibrils. *Proceedings of the National Academy of Sciences of the United States of America,* 102, 17342-17347.

LUNDMARK, K., WESTERMARK, G. T., OLSEN, A. & WESTERMARK, P. 2005. Protein fibrils in nature can enhance amyloid protein A amyloidosis in mice: Cross-seeding as a disease mechanism. *Proceedings of the National Academy of Sciences of the United States of America,* 102, 6098-6102.

LUO, Q., HOU, C. X., BAI, Y. S., WANG, R. B. & LIU, J. Q. 2016. Protein Assembly: Versatile Approaches to Construct Highly Ordered Nanostructures. *Chemical Reviews,* 116, 13571-13632.

MA, L. Z., LI, F., FANG, T., ZHANG, J. T. & WANG, Q. B. 2015. Controlled Self-Assembly of Proteins into Discrete Nanoarchitectures Templated by Gold Nanoparticles via Monovalent Interfacial Engineering. *ACS Applied Materials & Interfaces,* 7, 11024-11031.

MACPHEE, C. E. & DOBSON, C. M. 2000. Formation of mixed fibrils demonstrates the generic nature and potential utility of amyloid nanostructures. *Journal of the American Chemical Society,* 122, 12707-12713.

MADDELEIN, M. L. & WICKNER, R. B. 1999. Two prion-inducing regions of Ure2p are nonoverlapping. *Molecular and Cellular Biology,* 19, 4516-24.

MAJI, S. K., PERRIN, M. H., SAWAYA, M. R., JESSBERGER, S., VADODARIA, K., RISSMAN, R. A., SINGRU, P. S., NILSSON, K. P. R., SIMON, R., SCHUBERT, D., EISENBERG, D., RIVIER, J., SAWCHENKO, P., VALE, W. & RIEK, R. 2009. Functional Amyloids As Natural Storage of Peptide Hormones in Pituitary Secretory Granules. *Science,* 325, 328-332.

MALGAS, S., THORESEN, M., VAN DYK, J. S. & PLETSCHKE, B. I. 2017. Time dependence of enzyme synergism during the degradation of model and natural lignocellulosic substrates. *Enzyme and Microbial Technology,* 103**,** 1-11.
MANSFELD, J. & SCHELLENBERGER, A. 1987. Invertase immobilized on macroporous polystyrene: properties and kinetic characterization. *Biotechnology and Bioengineering,* 29**,** 72-78.
MASUTANI, K. & KIMURA, Y. 2015. Biobased Polymers. *In:* KOBAYASHI, S. & MÜLLEN, K. (eds.) *Encyclopedia of Polymeric Nanomaterials.* Berlin, Heidelberg: Springer Berlin Heidelberg.
MATOSEVIC, S., LYE, G. J. & BAGANZ, F. 2011. Immobilised enzyme microreactor for screening of multi-step bioconversions: characterisation of a de novo transketolase-omega-transaminase pathway to synthesise chiral amino alcohols. *Journal of Biotechnology,* 155**,** 320-329.
MCKENNA, S. M., LEIMKUHLER, S., HERTER, S., TURNER, N. J. & CARNELL, A. J. 2015. Enzyme cascade reactions: synthesis of furandicarboxylic acid (FDCA) and carboxylic acids using oxidases in tandem. *Green Chemistry,* 17**,** 3271-3275.
MCKITTRICK, J., CHEN, P. Y., BODDE, S. G., YANG, W., NOVITSKAYA, E. E. & MEYERS, M. A. 2012. The Structure, Functions, and Mechanical Properties of Keratin. *Jom,* 64**,** 449-468.
MEIER, C., LIFINCEV, I. & WELLAND, M. E. 2015. Conducting core-shell nanowires by amyloid nanofiber templated polymerization. *Biomacromolecules,* 16**,** 558-63.
MEISL, G., YANG, X. T., HELLSTRAND, E., FROHM, B., KIRKEGAARD, J. B., COHEN, S. I. A., DOBSON, C. M., LINSE, S. & KNOWLES, T. P. J. 2014. Differences in nucleation behavior underlie the contrasting aggregation kinetics of the A beta 40 and A beta 42 peptides. *Proceedings of the National Academy of Sciences of the United States of America,* 111**,** 9384-9389.
MEN, D., GUO, Y. C., ZHANG, Z. P., WEI, H. P., ZHOU, Y. F., CUI, Z. Q., LIANG, X. S., LI, K., LENG, Y., YOU, X. Y. & ZHANG, X. E. 2009. Seeding-Induced Self-assembling Protein Nanowires Dramatically Increase the Sensitivity of Immunoassays. *Nano Letters,* 9**,** 2246-2250.
MEN, D., ZHANG, Z. P., GUO, Y. C., ZHU, D. H., BI, L. J., DENG, J. Y., CUI, Z. Q., WEI, H. P. & ZHANG, X. E. 2010. An auto-biotinylated bifunctional protein nanowire for ultra-sensitive molecular biosensing. *Biosensors & Bioelectronics,* 26**,** 1137-1141.
MEN, D., ZHOU, J., LI, W., LENG, Y., CHEN, X. W., TAO, S. C. & ZHANG, X. E. 2016. Fluorescent Protein Nanowire-Mediated Protein Microarrays for Multiplexed and Highly Sensitive Pathogen Detection. *Acs Applied Materials & Interfaces,* 8**,** 17472-17477.
MICHAELS, T. C. T., SARIC, A., HABCHI, J., CHIA, S., MEISL, G., VENDRUSCOLO, M., DOBSON, C. M. & KNOWLES, T. P. J. 2018. Chemical Kinetics for Bridging Molecular Mechanisms and Macroscopic Measurements of Amyloid Fibril Formation. *Annual Review of Physical Chemistry,* 69**,** 273-298.
MICHELIN, M., PEIXOTO-NOGUEIRA, S. C., SILVA, T. M., JORGE, J. A., TERENZI, H. F., TEIXEIRA, J. A. & DE LOURDES T. M. POLIZELI, M. 2012. A novel xylan degrading β-d-xylosidase: purification and biochemical characterization. *World Journal of Microbiology and Biotechnology,* 28**,** 3179-3186.
MIN, K. & YOO, Y. J. 2014. Recent progress in nanobiocatalysis for enzyme immobilization and its application. *Biotechnology and Bioprocess Engineering,* 19**,** 553-567.
MITTAL, N., ANSARI, F., GOWDA, V. K., BROUZET, C., CHEN, P., LARSSON, P. T., ROTH, S. V., LUNDELL, F., WAGBERG, L., KOTOV, N. A. & SODERBERG, L. D. 2018. Multiscale Control of Nanocellulose Assembly: Transferring Remarkable Nanoscale Fibril Mechanics to Macroscale Fibers. *ACS Nano,* 12**,** 6378-6388.
MOHITE, B. V. & PATIL, S. V. 2014. A novel biomaterial: bacterial cellulose and its new era applications. *Biotechnology and Applied Biochemistry,* 61**,** 101-110.
NAKANO, M. & KAMINO, K. 2015. Amyloid-like Conformation and Interaction for the Self-Assembly in Barnacle Underwater Cement. *Biochemistry,* 54**,** 826-835.
NELSON, R. & EISENBERG, D. 2006. Structural models of amyloid-like fibrils. *Fibrous Proteins: Amyloids, Prions and Beta Proteins,* 73**,** 235-282.
NEVALAINEN, H. & PETERSON, R. 2014. Heterologous Expression of Proteins in Trichoderma. *Biotechnology and Biology of Trichoderma***,** 89-102.
NGO, S., GU, L. & GUO, Z. F. 2011. Hierarchical Organization in the Amyloid Core of Yeast Prion Protein Ure2. *Journal of Biological Chemistry,* 286**,** 29691-29699.

NGUYEN, P. Q., BOTYANSZKI, Z., TAY, P. K. R. & JOSHI, N. S. 2014. Programmable biofilm-based materials from engineered curli nanofibres. *Nature Communications,* 5**,** 1-10.
NICK MCELHINNY, S. A. & BECKER, J. J. 2014. Basic research opportunities focused on bio-based and bio-inspired materials and potential applications. *Frontiers in Chemistry,* 2**,** 24-27.
NOVOZYMES 2010. *Cellic CTec2 and HTec2 - Enzymes for hydrolysis of lignocellulosic materials*, (Luna No. 2010-01668-01).
NUSSBAUMER, M. G., NGUYEN, P. Q., TAY, P. K. R., NAYDICH, A., HYSI, E., BOTYANSZKI, Z. & JOSHI, N. S. 2017. Bootstrapped Biocatalysis: Biofilm-Derived Materials as Reversibly Functionalizable Multienzyme Surfaces. *ChemCatChem,* 9**,** 4328-4333.
NYSTROM, G., FERNANDEZ-RONCO, M. P., BOLISETTY, S., MAZZOTTI, M. & MEZZENGA, R. 2016. Amyloid Templated Gold Aerogels. *Adv Mater,* 28**,** 472-8.
PENG, D. F., YANG, J. C., LI, J., TANG, C. & LI, B. 2017. Foams Stabilized by beta-Lactoglobulin Amyloid Fibrils: Effect of pH. *Journal of Agricultural and Food Chemistry,* 65**,** 10658-10665.
PERCZEL, A., HUDAKY, P. & PALFI, V. K. 2007. Dead-end street of protein folding: thermodynamic rationale of amyloid fibril formation. *Journal of the American Chemical Society,* 129**,** 14959-14965.
PILKINGTON, S. M., ROBERTS, S. J., MEADE, S. J. & GERRARD, J. A. 2010. Amyloid Fibrils as a Nanoscaffold for Enzyme Immobilization. *Biotechnology Progress,* 26**,** 93-100.
QING, Q. & WYMAN, C. E. 2011. Supplementation with xylanase and β-xylosidase to reduce xylo-oligomer and xylan inhibition of enzymatic hydrolysis of cellulose and pretreated corn stover. *Biotechnology for Biofuels,* 4**,** 18-30.
RAYNES, J. K., PEARCE, F. G., MEADE, S. J. & GERRARD, J. A. 2011. Immobilization of Organophosphate Hydrolase on an Amyloid Fibril Nanoscaffold: Towards Bioremediation and Chemical Detoxification. *Biotechnology Progress,* 27**,** 360-367.
RISING, A. 2014. Controlled assembly: A prerequisite for the use of recombinant spider silk in regenerative medicine? *Acta Biomaterialia,* 10**,** 1627-1631.
SABATE, R., VILLAR-PIQUE, A., ESPARGARO, A. & VENTURA, S. 2012. Temperature Dependence of the Aggregation Kinetics of Sup35 and Ure2p Yeast Prions. *Biomacromolecules,* 13**,** 474-483.
SAKURABA, H., YOKONO, K., YONEDA, K., WATANABE, A., ASADA, Y., SATOMURA, T., YABUTANI, T., MOTONAKA, J. & OHSHIMA, T. 2010. Catalytic properties and crystal structure of quinoprotein aldose sugar dehydrogenase from hyperthermophilic archaeon Pyrobaculum aerophilum. *Archives of Biochemistry & Biophysics,* 502**,** 81-88.
SALEHI, S. & SCHEIBEL, T. 2018. Biomimetic spider silk fibres: From vision to reality. *The Biochemist.*
SATAM, C. C., IRVIN, C. W., LANG, A. W., JALLORINA, J. C. R., SHOFNER, M. L., REYNOLDS, J. R. & MEREDITH, J. C. 2018. Spray-Coated Multilayer Cellulose Nanocrystal—Chitin Nanofiber Films for Barrier Applications. *ACS Sustainable Chemistry & Engineering,* 6**,** 10637-10644.
SAVVIDES, N. & BELL, T. J. 1992. Microhardness and Young's modulus of diamond and diamondlike carbon films. *Journal of Applied Physics,* 72**,** 2791-2796.
SAWAYA, M. R., SAMBASHIVAN, S., NELSON, R., IVANOVA, M. I., SIEVERS, S. A., APOSTOL, M. I., THOMPSON, M. J., BALBIRNIE, M., WILTZIUS, J. J., MCFARLANE, H. T., MADSEN, A. O., RIEKEL, C. & EISENBERG, D. 2007. Atomic structures of amyloid cross-beta spines reveal varied steric zippers. *Nature,* 447**,** 453-457.
SCHEIBEL, T. 2005. Protein fibers as performance proteins: new technologies and applications. *Current Opinion in Biotechnology,* 16**,** 427-433.
SCHEIBEL, T., PARTHASARATHY, R., SAWICKI, G., LIN, X. M., JAEGER, H. & LINDQUIST, S. L. 2003. Conducting nanowires built by controlled self-assembly of amyloid fibers and selective metal deposition. *Proceedings of the National Academy of Sciences of the United States of America,* 100**,** 4527-4532.
SCHLEEGER, M., VANDENAKKER, C. C., DECKERT-GAUDIG, T., DECKERT, V., VELIKOV, K. P., KOENDERINK, G. & BONN, M. 2013. Amyloids: From molecular structure to mechanical properties. *Polymer,* 54**,** 2473-2488.
SEIBOTH, B., IVANOVA, C. & SEIDL-SEIBOTH, V. 2011. Trichoderma reesei: A Fungal Enzyme Producer for Cellulosic Biofuels. *Biofuel Production - Recent Developments and Prospects***,** 309-340.

SEONG, G. H., HEO, J. & CROOKS, R. M. 2003. Measurement of enzyme kinetics using a continuous-flow microfluidic system. *Analytical chemistry,* 75**,** 3161-3167.
SHEPARD, H. M., PHILLIPS, G. L., THANOS, C. D. & FELDNNANN, M. 2017. Developments in therapy with monoclonal antibodies and related proteins. *Clinical Medicine,* 17**,** 220-232.
SHIN, C. S., HONG, M. S., BAE, C. S. & LEE, J. 1997. Enhanced production of human mini-proinsulin in fed-batch cultures at high cell density of Escherichia coli BL21(DE3)[pET-3aT2M2]. *Biotechnology Progress,* 13**,** 249-257.
SHUKLA, A. A., HUBBARD, B., TRESSEL, T., GUHAN, S. & LOW, D. 2007. Downstream processing of monoclonal antibodies - Application of platform approaches. *Journal of Chromatography B-Analytical Technologies in the Biomedical and Life Sciences,* 848**,** 28-39.
SMITH, J. F., KNOWLES, T. P. J., DOBSON, C. M., MACPHEE, C. E. & WELLAND, M. E. 2006. Characterization of the nanoscale properties of individual amyloid fibrils. *Proceedings of the National Academy of Sciences of the United States of America,* 103**,** 15806-15811.
SOTO, C. M. 2014. Protein engineering and other bio-synthetic routes for bio-based materials: current uses and potential applications. *Frontiers in Chemistry,* 2**,** 83.
SOUTHALL, S. M., DOEL, J. J., RICHARDSON, D. J. & OUBRIE, A. 2006. Soluble aldose sugar dehydrogenase from Escherichia coli - A highly exposed active site conferring broad substrate specificity. *Journal of Biological Chemistry,* 281**,** 30650-30659.
SPOHNER, S. C., MULLER, H., QUITMANN, H. & CZERMAK, P. 2015. Expression of enzymes for the usage in food and feed industry with Pichia pastoris. *Journal of Biotechnology,* 202**,** 118-134.
STATHOPULOS, P. B., SCHOLZ, G. A., HWANG, Y. M., RUMFELDT, J. A. O., LEPOCK, J. R. & MEIERING, E. M. 2004. Sonication of proteins causes formation of aggregates that resemble amyloid. *Protein Science,* 13**,** 3017-3027.
SU, X. Y., SCHMITZ, G., ZHANG, M. L., MACKIE, R. I. & CANN, I. K. O. 2012. Heterologous Gene Expression in Filamentous Fungi. *Advances in Applied Microbiology, Vol 81,* 81**,** 1-61.
SUN, X. S. 2005. Overview of Plant Polymers: Resources, Demands, and Sustainability. *In:* WOOL, R. P. & SUN, X. S. (eds.) *Bio-Based Polymers and Composites.* Burlington: Academic Press.
TAMAMIS, P., ADLER-ABRAMOVICH, L., RECHES, M., MARSHALL, K., SIKORSKI, P., SERPELL, L., GAZIT, E. & ARCHONTIS, G. 2009. Self-Assembly of Phenylalanine Oligopeptides: Insights from Experiments and Simulations. *Biophysical Journal,* 96**,** 5020-5029.
TIWARI, R., NAIN, L., LABROU, N. E. & SHUKLA, P. 2018. Bioprospecting of functional cellulases from metagenome for second generation biofuel production: a review. *Critical Reviews in Microbiology,* 44**,** 244-257.
TOYAMA, B. H. & WEISSMAN, J. S. 2011. Amyloid Structure: Conformational Diversity and Consequences. *Annual Review of Biochemistry,* 80**,** 557-585.
URBAN, P. L., GOODALL, D. M. & BRUCE, N. C. 2006. Enzymatic microreactors in chemical analysis and kinetic studies. *Biotechnology Advances,* 24**,** 42-57.
VARGHESE, A. M. & MITTAL, V. 2018. Polymer composites with functionalized natural fibers. *In:* SHIMPI, N. G. (ed.) *Biodegradable and Biocompatible Polymer Composites.* Woodhead Publishing.
VEHOFF, T., GLISOVIC, A., SCHOLLMEYER, H., ZIPPELIUS, A. & SALDITT, T. 2007. Mechanical properties of spider dragline silk: Humidity, hysteresis, and relaxation. *Biophysical Journal,* 93**,** 4425-4432.
WAKU, T. & TANAKA, N. 2017. Recent advances in nanofibrous assemblies based on -sheet-forming peptides for biomedical applications. *Polymer International,* 66**,** 277-288.
WALLER, C. L., GRIFFITHS, H. J., WALUDA, C. M., THORPE, S. E., LOAIZA, I., MORENO, B., PACHERRES, C. O. & HUGHES, K. A. 2017. Microplastics in the Antarctic marine system: An emerging area of research. *Science of the Total Environment,* 598**,** 220-227.
WANG, Y., PU, J., AN, B., LU, T. K. & ZHONG, C. 2018. Emerging Paradigms for Synthetic Design of Functional Amyloids. *Journal of Molecular Biology,* 430**,** 3720-3734.
WEBBER, M. J., APPEL, E. A., MEIJER, E. W. & LANGER, R. 2015. Supramolecular biomaterials. *Nature Materials,* 15**,** 13+26.
WEI, G., SU, Z. Q., REYNOLDS, N. P., AROSIO, P., HAMLEY, I. W., GAZIT, E. & MEZZENGA, R. 2017. Self-assembling peptide and protein amyloids: from structure to tailored function in nanotechnology. *Chemical Society Reviews,* 46**,** 4661-4708.

WESTERS, L., WESTERS, H. & QUAX, W. J. 2004. Bacillus subtilis as cell factory for pharmaceutical proteins: a biotechnological approach to optimize the host organism. *Biochimica Et Biophysica Acta-Molecular Cell Research,* 1694**,** 299-310.
WHITFORD, D. 2005. *Proteins: Structure and Function*, Wiley.
WILLIAMS, D. 2014. *Essential Biomaterial Science*, Cambridge University Press, Cambridge.
WOOLFSON, D. N. & MAHMOUD, Z. N. 2010. More than just bare scaffolds: towards multi-component and decorated fibrous biomaterials. *Chemical Society Reviews,* 39**,** 3464-3479.
WRIGHT, S. L. & KELLY, F. J. 2017. Plastic and Human Health: A Micro Issue? *Environmental Science & Technology,* 51**,** 6634-6647.
YAGHI, O. M., O'KEEFFE, M., OCKWIG, N. W., CHAE, H. K., EDDAOUDI, M. & KIM, J. 2003. Reticular synthesis and the design of new materials. *Nature,* 423**,** 705-714.
YANG, X. Z., SHI, P. J., HUANG, H. Q., LUO, H. Y., WANG, Y. R., ZHANG, W. & YAO, B. 2014. Two xylose-tolerant GH43 bifunctional beta-xylosidase/alpha-arabinosidases and one GH11 xylanase from Humicola insolens and their synergy in the degradation of xylan. *Food Chemistry,* 148**,** 381-387.
YE, X., JUNEL, K., GÄLLSTEDT, M., LANGTON, M., WEI, X.-F., LENDEL, C. & HEDENQVIST, M. S. 2018. Protein/Protein Nanocomposite Based on Whey Protein Nanofibrils in a Whey Protein Matrix. *ACS Sustainable Chemistry & Engineering,* 6**,** 5462-5469.
ZAMBRANO, R., CONCHILLO-SOLE, O., IGLESIAS, V., ILLA, R., ROUSSEAU, F., SCHYMKOWITZ, J., SABATE, R., DAURA, X. & VENTURA, S. 2015. PrionW: a server to identify proteins containing glutamine/asparagine rich prion-like domains and their amyloid cores. *Nucleic Acids Research,* 43**,** W331-W337.
ZHANG, K., SU, L. Q., DUAN, X. G., LIU, L. N. & WU, J. 2017. High-level extracellular protein production in Bacillus subtilis using an optimized dual-promoter expression system. *Microbial Cell Factories,* 16**,** 1-15.
ZHANG, R. C., YANG, Y. K., HUANG, C. H., ZHAO, L. & SUN, P. Z. 2016. Kinetics and modeling of sulfonamide antibiotic degradation in wastewater and human urine by UV/H2O2 and UV/PDS. *Water Research,* 103**,** 283-292.
ZHONG, C., GURRY, T., CHENG, A. A., DOWNEY, J., DENG, Z. T., STULTZ, C. M. & LU, T. K. 2014. Strong underwater adhesives made by self-assembling multi-protein nanofibres. *Nature Nanotechnology,* 9**,** 858-866.
ZHOU, X. M., ENTWISTLE, A., ZHANG, H., JACKSON, A. P., MASON, T. O., SHIMANOVICH, U., KNOWLES, T. P. J., SMITH, A. T., SAWYER, E. B. & PERRETT, S. 2014. Self-Assembly of Amyloid Fibrils That Display Active Enzymes. *ChemCatChem,* 6**,** 1961-1968.
ZHOU, X. M., SHIMANOVICH, U., HERLING, T. W., WU, S., DOBSON, C. M., KNOWLES, T. P. J. & PERRETT, S. 2015. Enzymatically Active Microgels from Self-Assembling Protein Nanofibrils for Microflow Chemistry. *ACS Nano,* 9**,** 5772-5781.
ZHOU, Z. & HARTMANN, M. 2013. Progress in enzyme immobilization in ordered mesoporous materials and related applications. *Chemical Society Reviews,* 42**,** 3894-3912.

Popular Science Summary

Proteins are large biomolecules, which are the basic building blocks of life. In fact, proteins steer cellular and intracellular functions, accelerate biochemical reactions, and act as signal transducers. Another important function of proteins is that these biomolecules can be assembled into different materials. These materials possess a large range of properties, which vary from rigid to elastic. Due to the versatility of protein materials they are used for many different purposes. Among others, proteins are building blocks of hair, nail, bone and skin.

A protein is a long chain of covalently bound aminoacids, which fold into well-defined 3D structures. The 3D-structure determines the function of a protein. However, these constructs are rather fragile, which means that proteins are prone to refold and aggregate. To prevent this from happening, advanced cellular security mechanisms take care of misfolded proteins. However, mutations, stress and failure of the security mechanisms result in accumulation of aggregated proteins in vital organs. This is the cause for severe diseases that are more likely to occur at an advanced age and limits the quality of life. Most common diseases are Alzheimer's, Parkinson's, and diabetes type II.

In the beginning of this millennium, new data suggested that these aggregates consist of highly ordered, nanosized fibrils. Then, researchers also discovered that protein nanofibrils are not only the origin of diseases, but that the high stability of these aggregates are utilized by simple microorganisms, and also by higher multicellular organisms including humans. This insight was the key to recognize the enormous potential of the fibrils for biotechnological applications.

From material point of view, the mechanical strength of the fibrils is comparable to spider silk, 'natures high performance polymer'. Due to the small size of the protein fibrils – the diameter is 10,000 times thinner than a human hair – they have a really large surface area, which makes them attractive for all kind of applications. Since proteins are designable by changing the DNA sequence, likewise the fibril properties can be adjusted through the genetic code. This makes it possible to decorate the fibrils with other proteins that perform a

specific function, without using chemistry. Therefore, the protein nanofibrils, are also a very promising material from an environmental perspective. In principle, only microorganisms are necessary to produce the fibrils.

In this work I have assembled fibrils that can be used as a material to purify antibodies, if developed further. The significance of this finding is that monoclonal antibodies are a new class of medication that aim to activate the innate immune systems, in order to reduce common side effects that are typical for small compound drugs. The demand for these therapeutically antibodies increases at an astonishing rate, which requires new, faster and cheaper ways to purify them. A possible solution to this new demand are my antibody binding fibrils that have a 5-time increased binding capacity, compared to any existing commercially available product.

Antibiotic contaminations are another severe concern that threatens the effectiveness of future healthcare. Minor antibiotic contaminations in the environment can result in the development of resistances of pathological microorganisms against these anti-microbial agents. Chemical methods that degrade antibiotics are not 100 % efficient, and could produce unwanted by-products. Therefore, I developed a biochemical method that employs enzymes which are linked to the protein nanofibrils instead. In this study I was also able to show that the enzyme linked to the fibril has the same catalytic efficiency as the normal enzyme in solution.

To utilize renewable resources and consequentially reduce the dependency of our society on petrol-based products is another research area that is very famous. Yet again, I have developed fibrils that are linked to a cascade of enzymes, which makes the enzymes reusable. I have also successfully tested to process biomass from beechwood using the enzymatic fibril cascade. This method could be an important step towards making biomass utilization cheaper.

The large-scale production of the fibrils is a big concern, and one of the reasons why none of the fibrils reported in scientific literature have reached commercial maturity yet. The transition from the laboratory to the real-world application is not a simple task, which requires a lot of work that goes beyond basic research. As a first step towards this end goal, have genetically engineered a yeast that produces functional nanofibrils in the cultivation medium. After cultivation the fibrils are ready-to-use and need only to be rinsed with water to completely remove the yeast cells. This method still requires some optimization, but is definitely appropriate for upscaling.

Acknowledgements

The past years were an incredible journey that was made possible by the support of many people. Therefore, I would like to dedicate this last section of my thesis to thank everyone who has helped me to make this thesis a reality.

First, I would like to express my appreciation to my supervisors, who have always provided an excellent support and shared their knowledge with me. *Torleif Härd* recruited me and introduced me to the exciting world of functional protein materials. I am really grateful for this opportunity and also for his excellent feedback and encouragement. *Mats Sandgren* has guided me through the process of publishing. I especially appreciate that he helped me to refocus and gather my thoughts when experiments did not work the way they were 'supposed' to! Also, I want to thank *Jerry Ståhlberg*, in particular for the incredible X-Ray crystallography course, the best course that I took during my PhD education.

I would like to thank my co-authors and collaborators for their constant efforts and their problem-solving skills. I appreciated the many scientific discussions with *Henrik Hansson*, *Johanna Blomqvist* and *Mikael Gudmundsson*. Thank you *Mahafuzur Rahman***,** for all the conversations on anything that has to do with life as a PhD, as well as science related discussions. I really enjoyed our close collaboration and hope that this work will eventually be published. A special thank you to *Jan Eriksson,* who helped me with the mass spectrometry experiments and the staff at the BioVis facility for providing the TEM images of my fibrils.

I want to thank all my co-workers at the department, that made life in the lab an enjoyable time. In particular I want express my appreciation for past and present PhD students, post docs, and researchers that I have shared the lab with. Thank you, for being extraordinary colleagues! There was always someone that I could

ask for assistance (especially *Nils Mikkelsen* - who knows how to fix everything), which contributed to a pleasant working environment.

Finally, I would like to thank my *family* for their love and constant support!